

Fine-Grained and Real-Time Gesture Recognition by Using IMU Sensors

Dian Zhang^{ID}, Member, IEEE, Zexiong Liao^{ID}, Wen Xie^{ID}, Xiaofeng Wu^{ID}, Haoran Xie^{ID}, Senior Member, IEEE, Jiang Xiao^{ID}, and Landu Jiang^{ID}

Abstract—Gesture recognition by using Inertial Measurement Unit (IMU) sensors plays an important role in various Internet of Things (IOT) applications, e.g., smart home, intelligent medical system and so on. Traditional technologies usually utilize machine learning algorithms to train different gestures during the offline phase, then recognize the gesture during the online phase. However, such technologies cannot recognize these gestures without prior training. Even for the same gesture, with different gesture amplitude may result in unsuccessful recognition. Also if we change the person to perform the same gesture, the algorithms fails. In order to overcome these drawbacks, we propose an approach, which will be able to track the human body motion in real-time and also recognize complicated gestures. It utilizes the accelerometer information and proposes comprehensive localization algorithms for each deployed sensor attached on the human body. Then, it takes the correlation and limitation among body parts into account to recognize the gesture. Our experiments results show that, the successful recognition rate of our algorithm is 100%. Furthermore, any part of the human body can be well tracked, the tracking accuracy can reach 0.06m.

Index Terms—IMU, gesture recognition, motion tracking

1 INTRODUCTION

GESTURE recognition using wireless technologies plays an important role in many applications. For example, various Virtual Reality (VR) applications and products require to show the human's gesture in the virtual world [1], [2]. In the smart home applications [3], [4], the human gestures recognition is quite useful to decide how to control these intelligent devices. In the intelligent medical system [5], [6], users may utilize gesture recognition to discover the patient motion behavior and their intention easily. Compared to traditional vision-based technologies [2], [7], [8]. Wireless technologies are not limited by line of sight or light condition of the devices. Furthermore, user privacy can be protected using such technologies. Thus, gesture recognition using wireless technologies attract the attention of many researchers.

Among current gesture recognition based on wireless technologies, some utilize WiFi or other device to detect the signals influenced by the target [9], [10], [11]. But the signals

are easily affected by the surroundings, causing the accuracy to vary the accuracy vary easily. Some other technologies adopt wearable devices, e.g., Inertial Measurement Unit (IMU) sensors. However, such gesture recognition algorithms usually utilize machine learning algorithms to train some data set during the offline phase, then run it during the online phase [12], [13], [14]. These method can only recognize common human gestures. If new gesture occurs, these recognition algorithms tend to fail easily. Even for the same gesture that has already been trained, different gesture amplitude may result in failure to recognize. Also if we change the person to perform the same gesture, the algorithms will fail easily.

In order to overcome these drawbacks introduced earlier, we propose an approach base on IMU sensors, which will be able to recognize various human gestures having different amplitude precisely in real time, without having to train during the offline phase. The added advantage is that complicated gestures can also be recognized.

Our basic idea is to utilize the accelerometer information to localize each deployed sensor on the human body. Our algorithms not only can refine the hardware linear distortion, but also can eliminate the impact of the gravity and hardware differences. Furthermore, the correlation between the deployed sensors on human body also utilized to refine the tracking results. As a result, we may easily recognize different human gestures and track human body motion. Even for the same human body gestures with different amplitudes, our algorithm is able to recognize and differentiate them easily.

To sum up, the contribution of our paper is listed as below.

- 1) Our proposed approach can precisely recognize the human gestures with different amplitude and also track body motion;

• Dian Zhang, Zexiong Liao, Wen Xie, and Landu Jiang are with the Shenzhen University, Shenzhen 518060, China. E-mail: serena.dian@gmail.com, {1810273017, 1810273027}@email.szu.edu.cn, landu.jiang@mail.mcgill.ca.

• Xiaofeng Wu is with the Shenzhen Research Institute of Big Data, Shenzhen 518172, China. E-mail: 867746816@qq.com.

• Haoran Xie is with the Lingnan University, Hong Kong. E-mail: hrchie@ln.edu.hk.

• Jiang Xiao is with the Huazhong University of Science and Technology, Wuhan, Hubei 430074, China. E-mail: jiangxiao@hust.edu.cn.

Manuscript received 20 November 2020; revised 24 September 2021; accepted 28 September 2021. Date of publication 30 November 2021; date of current version 6 March 2023.

This work was supported in part by the NSFC under Grant 61872247, in part by the Shenzhen Peacock Talent under Grant 827-000175, and in part by the Guangdong Natural Science Funds under Grant 2019A1515011064.

(Corresponding authors: Jiang Xiao and Landu Jiang.)

Digital Object Identifier no. 10.1109/TMC.2021.3120475

通过使用IMU传感器的细粒度和实时手势识别

Dian Zhang, IEEE, Zexiong Liao, Wen Xie, Xiaofeng Wu, Haoran Xie, IE
EE, Jiang Xiao和Landu Jiang的高级会员

摘要 - 使用惯性测量单元 (IMU) 传感器通过使用智能互联网 (IoT) 应用程序（例如智能家居，智能医疗系统等）中识别的良好识别。传统技术通常利用机器学习算法在阶段训练不同的手势，然后在线阶段识别手势。但是，如果没有事先培训，这些技术就无法识别这些手势。即使以相同的手势，具有不同的手势振幅也可能导致识别失败。另外，如果我们更改人员执行相同的手势，则算法会失败。为了克服这些缺点，我们提出了一种方法，该方法将能够实时跟踪人体运动并认识到复杂的手势。它利用加速度计的信息，并建议针对人体附着的每个部署的传感器进行全面的定位算法。然后，它考虑了身体部位之间的相关性和限制，以识别手势。我们的实验结果表明，我们算法的成功识别率为100%。此外，人体的任何部分都可以很好地跟踪，跟踪精度可以达到0: 06m。

索引术语 - IMU, 手势识别, 运动跟踪

1简介

使用无线技术的手势识别在许多应用中起着重要作用。例如，各种虚拟现实 (VR) 应用和产品需要在虚拟世界中显示人类的手势[1], [2]。在智能家庭应用[3], [4]中，人类的手势识别对于决定如何控制这些智能设备非常有用。在智能医疗系统[5], [6]中，用户可以使用手势识别来发现患者的运动行为及其意图。与传统的基于视觉的技术相比[2], [7], [8]。无线技术不受视线或偏见状态的限制。此外，可以使用此类技术保护用户隐私。因此，使用无线技术的手势识别引起了许多研究人员的注意。

在基于无线技术的当前手势识别中，有些使用WiFi或其他设备来检测目标[9], [10], [11]所影响的信号。但是信号

很容易受到周围环境的影响，导致准确性变化很容易变化。其他一些技术采用可穿戴设备，例如惯性测量单元 (IMU) 传感器。但是，这种手势识别算法通常会利用机器学习算法在途中训练一些数据集，然后在在线阶段[12], [13], [14]中运行它。这些方法只能识别共同的人类手势。如果发生新的手势，这些认可算法往往容易失败。即使对于已经经过训练的同一阶段，不同的手势振幅也可能导致未能识别。另外，如果我们将人更改为同样的手势，则算法将很容易失败。

为了克服前面引入的这些缺点，我们提出了IMU传感器的方法基础，该方法将能够识别出具有不同振幅的各种人类手势，而无需在阶段训练。额外的优势是，也可以识别合并的手势。

我们的基本思想是利用加速度计信息来将每个部署的传感器定位在人体上。我们的算法不仅可以重新确定硬件线性失真，还可以消除重力和硬件差异的影响。此外，人体部署传感器之间的相关性也用于重新填充跟踪结果。结果，我们很容易认识到不同的人类手势并跟踪人体运动。即使对于具有不同振幅的相同人体手势，我们的算法也能够轻松识别和区分它们。

总而言之，我们的论文的贡献如下所示。

- 1) 我们提出的方法可以精确地识别人类手势不同的振幅并跟踪身体运动；

• Dian Zhang, Zexiong Liao, Wen Xie, and Landu Jiang are with the Shenzhen University, Shenzhen 518060, China. E-mail: serena.dian@gmail.com, {1810273017, 1810273027}@email.szu.edu.cn, landu.jiang@mail.mcgill.ca.

• Xiaofeng Wu is with the Shenzhen Research Institute of Big Data, Shenzhen 518172, China. E-mail: 867746816@qq.com.

• Haoran Xie is with the Lingnan University, Hong Kong. E-mail: hrxie@ln.edu.hk.

• Jiang Xiao is with the Huazhong University of Science and Technology, Wuhan, Hubei 430074, China. E-mail: jiangxiao@hust.edu.cn.

Manuscript received 20 November 2020; revised 24 September 2021; accepted 28 September 2021. Date of publication 30 November 2021; date of current version 6 March 2023.

This work was supported in part by the NSFC under Grant 61872247, in part by the Shenzhen Peacock Talent under Grant 827-000175, and in part by the Guangdong Natural Science Funds under Grant 2019A1515011064. (Corresponding authors: Jiang Xiao and Landu Jiang.)

Digital Object Identifier no. 10.1109/TMC.2021.3120475

- 2) Compared to traditional technologies, our algorithms can be performed without prior training, making it to be widely used in real scenarios, like virtual reality or interactive game;
- 3) We utilize the limitation of the body motion and the correlation among the body parts to improve the accuracy of the gesture recognition and motion tracking.

Our experiments are based on IMU sensors, each includes a 3-axis accelerometer, a 3-axis gyroscope and 3-axis Compass. These sensors are deployed on different parts of the human bodies. After 40 rounds of different gesture tests, experiment results show that the successfully recognition rate of our algorithm is 100%. Furthermore, the average localization error of all the deployed sensors is only 0.06 m.

The rest of this paper is organized as follows. We will introduce the related work in the Section 2. Section 3 contains details of our methodology. The implementation of our experiment and accuracy of the recognition will be presented at Section 4. Finally, we will conclude this paper and point our future work.

2 RELATED WORK

2.1 Gesture Recognition Technology

Tradition gesture recognition technologies basically can be classified into 4 categories: vision based technologies, radio technologies, wearable device technologies and hybrid technologies.

1. Vision based technologies utilize the cameras to capture the gesture by applying various image processing algorithms [15], [16], [17]. Juang [18] is able to classify the human body gesture using an interval type-2 neural fuzzy classifier. Ohn-Bar [19] can recognize driver hand gestures by employing a combined RGB and depth descriptor. Brulin [20] leveraged fuzzy logic to recognize 4 static gestures for elderly. Ren [21] utilized Kinect sensors and proposed a Finger-Earth Mover's Distance (FEMD) metric to measure the difference between different hand shapes, it can reach a high accuracy based on a dataset of 10 gestures. Ju *et al.* [22] purposed a integrative framework to segment hand gestures using the Kinect device. Kevin *et al.* [23] have developed hand gestures recognition based on Kinect camera using Histogram of Oriented Gradient (HOG) and Dynamic Time Warping (DTW) methods. There are some work utilize Leap Motion controller to recognize gesture [24], [25], [26]. These works usually require light for the environment. Furthermore, the camera has a limited covering area. The privacy problem is also a concern.

2. Radio technologies are popular since they have no light limitation and privacy concern. In such technologies, usually a number of various wireless devices are utilized, e.g., the WiFi devices [9], [10]. Activity recognition and monitoring system (CARM) [9] is able to recognize device-free human target activity based on the Channel State Information (CSI) signals difference caused by the target. In the CARM, Hidden Markov Model (HMM) is used to build the activity model. He [10] proposed a device-free gesture recognition system based on WiFi infrastructure and devices. Wang *et al.* [27] utilized the mmWave signals to realize gesture recognition. However, when signals are blocked by obstacles (Non-Line-of-Sight signals [28]), the accuracy of

recognition will be reduced. WiTrack [29] can track the 3D motion of a user from the radio signals reflected by the human body. But it only can provide coarse tracking of body parts. Pantomime [30] can realize gesture recognition through millimeter-wave radio frequency signals. But it has lower accuracy if gestures are performed along the Z axis and the gestures should be performed at slow speed. Widar3.0 [31] is a Wi-Fi based zero-effort cross-domain gesture recognition system. But different user heights will influence the gesture recognition rate.

3. A large number of works aim to recognize target gestures using the wearable devices. Among them, technologies based on IMU devices [12], [32], [33], [34] are most popular. The IMU sensors include an accelerometer and a gyroscope. Jerome [35] utilized a neural network algorithm to recognize gestures wearing smart gloves, but it is only limited to static gestures. Xu [32] utilized the IMU sensors and proposed an automatic gesture segmentation algorithm, which is developed to identify individual gestures in a sequence to recognize seven hand gestures. Wu [12] utilized arm orientation limitation and joint angle to refine the gesture model. However, the above technologies can only estimate the likelihood of a number of predefined gestures and cannot recognize the same gestures with different amplitude. S.H.P [36] utilized a micro-inertial sensor and a three-axis magnetometer to propose a tracking tool system. This system mainly correct the position of the tool. Gupta [37] proposed a continuous gesture recognition algorithm, which mainly uses the IMU sensors on the mobile phone to compress and encode each gesture. It aims to mark the start and end of each gesture, then achieves a continuous gesture recognition. However, this algorithm only recognizes predefined gestures. Yun's work [38] is able to track the human body motion in real-time by using angular rate sensor and accelerometer sensor. However, it utilized the angular motion of the body (limb) to recognize simple gestures, but it cannot recognize complicated gestures, e.g., having both displacement and rotation. The continuous hand gesture recognition methodology [37] utilized the IMU sensors. This methodology detected the start and end points of meaningful gesture segments, then used the DTW algorithm to identify a gesture. However, it can only recognize gestures that have been categorized in advance.

There are also some technologies based on other wearable device proposed in recent years. Watanabe *et al.* [39] utilized sound wave to recognize gestures and proposed a method to improve ultrasound-based gesture recognition by attaching a cover to the microphone. Zhang *et al.* [40] proposed a gesture input technique using Photoplethysmography (PPG) signal that optical heart-rate sensors capture. They utilized optical sensors on the off-the-shelf wearable devices to recognise gestures. Becker *et al.* [41] utilized a wireless electromyography (EMG) armband to classify the finger touches and estimates their force. Zhang *et al.* [42] proposed a novel gesture recognition framework to learn intrinsic spatial and temporal features of surface electromyography (sEMG). But these methods are either with higher cost or inconvenient to use.

4. Some researchers used hybrid technologies in gesture recognition. Chan *et al.* [43] designed a hand tracking glove. It employed sensing data from three different sensors, which

- 2) 与传统技术相比，我们的算法可以在没有事先培训的情况下执行，从而在实际场景中广泛使用，例如虚拟现实或互动游戏；
- 3) 我们利用身体运动的局限性和身体部位之间的相关性，以改善手势识别和运动跟踪的认可。

我们的实验基于IMU传感器，每个传感器包括3轴加速度计，3轴陀螺仪和3轴指南针。这些传感器部署在人体的不同部位上。经过40轮不同的手势测试后，实验结果表明，我们算法的成功识别率为100%。此外，所有部署传感器的平均本地化误差仅为0.06 m。

本文的其余部分如下组织。我们将在第2节中介绍相关工作。第3节包含我们方法论的详细信息。我们的实验和认可准确性的实施将在第4节中进行。最后，我们将结束本文并指出未来的工作。

2 相关工作

2.1 手势识别技术

传统手势识别技术基本上可以分为4个类别：基于视觉的技术，无线电技术，可穿戴设备技术和混合技术。

1. 基于视觉的技术，利用摄像机通过应用各种图像处理算法[15], [16], [17]来限制手势。Juang [18]能够使用间隔2型神经模糊分类器对人体手势进行分类。OHN-BAR [19]可以通过使用组合的RGB和深度描述符来识别驾驶员手势。Brulin [20]利用模糊逻辑来识别4个老年人的静态手势。Ren [21]利用了Kinect传感器，并提出了一个芬格 - 地球Movera - s距离(femd)度量，以测量不同手形之间的差异，它可以基于10个手势的数据集达到高精度。Ju等。[22]目的是使用Kinect设备进行分段手工盖的综合框架。凯文等。[23]使用定向梯度(HOG)和动态时间扭曲(DTW)方法的直方图，具有基于Kinect摄像机的开发手势识别。有一些工作利用LEAP运动控制器来识别手势[24], [25], [26]。这些作品通常需要环境光。摄像机的覆盖面积有限。审核问题也是一个问题。

2. 无线电技术很受欢迎，因为它们没有光限制和隐私问题。在这样的技术中，通常使用许多各种无线设备，例如WiFi设备[9], [10]。活动识别和监测系统(CARM) [9]能够基于基于目标引起的通道状态信息(CSI)信号差异识别无装置的人类目标活动。在卡姆中，隐藏的马尔可夫模型(HMM)用于构建活动模型。他[10]提出了一个基于WiFi基础架构和设备的无设备手势接收系统。Wang等。[27]利用MMWave信号实现了识别。但是，当信号被障碍物阻塞(非线信号[28])时

识别将减少。Witrack [29]可以从人体反映的无线电信号中跟踪用户的3D运动。但是它只能提供对身体部位的粗略跟踪。Pantomime [30]可以通过毫米波射频信号实现手势识别。但是，如果沿Z轴进行手势，并且应以缓慢的速度执行手势，则其精度较低。WIDAR3.0 [31]是基于Wi-Fi的零富特性跨域识别系统。但是不同的用户高度会影响手势识别率。

3. 大量作品旨在使用可穿戴设备来识别目标套件。其中，基于IMU设备的技术[12], [32], [33], [34]最受欢迎。IMU传感器包括加速度计和陀螺仪。Jerome [35]利用神经网络算法来识别戴着智能手套的手势，但仅限于静态手势。Xu [32]使用了IMU传感器，并提出了自动手势分割算法算法，该算法是为了识别序列中的单个手势以识别七个手势的手势。Wu [12]利用了Arm方向限制和关节角度重新确定手势模型。但是，上述技术只能估算出许多预定的手势的可能性，并且无法以不同的幅度识别相同的手势。S.H.P [36]使用微惯性传感器和三轴磁力计提出了跟踪工具系统。该系统主要纠正工具的位置。Gupta [37]提出了一种连续的手势识别算法，该算法主要使用手机上的IMU传感器来压缩和编码每个手势。它旨在标记每个手势的开始和结束，然后获得连续的手势识别。但是，该算法仅识别预定的手势。Yun的工作[38]能够使用角度速率传感器和加速度计传感器实时跟踪人体运动。但是，它利用身体(肢体)的角运动来识别简单的手势，但无法识别复杂的手势，例如具有位移和旋转。连续的手势识别方法[37]使用了IMU传感器。该方法检测到有意义的手势段的起点和终点，然后使用DTW算法来识别手势。但是，它只能识别已提前分类的手势。

近年来，还有一些基于其他能够磨损设备的技术。渡边等人。[39]利用声波来识别手势，并提出了一种通过将盖子连接到麦克风上来改善基于超声的手势识别的方法。张等。[40]提出了一种使用光插曲(PPG)信号的手势输入技术，该信号是光学心率传感器盖的。他们在现成的可穿戴设备上使用光传感器来识别手势。贝克等人。[41]UTI-LIZ-LIZE无线肌电图(EMG)臂章，以使纤维触摸并估计其力。张等。[42]提出了一个新型的手势识别框架，以学习表面电子学(SEMG)的内在空间和时间特征。但是这些方法要么具有更高的成本或不便。

4. 一些研究人员在手势识别中使用了混合技术。Chan等。[43]设计了一个手跟踪手套。它采用了来自三个不同传感器的传感数据，

includes a camera, an IMU and flex sensors. Besides, the Kalman filter is applied to stabilize the pose acquired. These technologies requires various devices to be deployed and are inconvenient to use in practice.

2.2 Gesture Recognition Algorithms

There are huge amount of work [44], [45], [46], [47], [48], [49], [50], [51] leveraging machine learning algorithms to recognize the human gestures. Zhu and Sheng [48] utilized the Neural Network and Hidden Markov Model to recognize gesture. Zhao [49] proposed a real-time gesture recognition system for head-mounted devices. This system mainly trained the collected head motion information to establish a hidden Markov Model, then recognized the gesture in real time. Wang and Chuang [46] utilizes Linear Discriminant Analysis (LDA) to extract feature and employ Probabilistic Neural Network (PNN) to recognize gestures. Wu and Sun [50] utilized the muscle sensors and inertial sensors to collect the gesture data of sign language, then used the Support Vector Machine (SVM), Naive Bayes (NB) and K-Nearest Neighbor (KNN) algorithm to classify the gestures. Bhuyan [51] utilized the gyroscope and accelerometer to predict the direction of rotation of the arm, then uses Kalman filtering to find the exact position of the arm. Wang *et al.* [27] developed tow Generative Adversarial Networks (GANs), i.e., SS-GAN and ST-GAN, to improve human gesture recognition accuracy. Zhang *et al.* [42] designed a convolutional recurrent neural network (CRNN) architecture to identify hand gestures. Gochoo *et al.* [52] proposed an IoT-based privacy-preserving yoga posture recognition system employing a deep convolutional neural network (DCNN).

However, these machine learning algorithms are only able to recognize gestures already trained during the offline phase. If a different gesture occurs, or the target human has been replaced, or even the same person performs same gesture but with different amplitude, these methodologies usually fail to recognize them. Therefore, machine learning algorithms only can recognize limited number of pre-defined gestures. Especially, their training cost is high.

In our work, we can accurately recognize complicate gestures in real time, even if gestures are similar but with different amplitude. Compared to machine learning algorithms, our algorithms do not require high computational costs and can be performed without prior training.

3 METHODOLOGY

In our approach, we first eliminate the noise and linear distortion of the hardware devices, then eliminate the impact of gravity on such data. In the following, we propose a comprehensive algorithm to track human gesture in real time, which can eliminate the hardware sensitivity difference and effectively utilize limitation of body motion to improve the tracking accuracy dramatically. Finally, we propose a recognition algorithm to recognize human body gesture.

3.1 Gyroscope Noise Reduction

The gyroscope sensor mainly consists of three kinds of errors. The first error is the high-frequency noise. The second error is the linear distortion of the hardware caused by the welding inaccuracy, plane curvature and roughness, as well as circuit

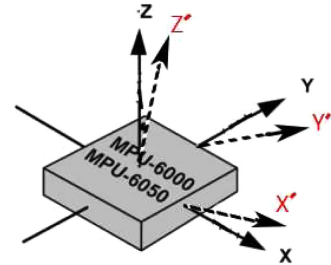


Fig. 1. Hardware linear distortion. x , y and z axis are the ideal state, while x' , y' and z' are the actual state.

board processing accuracy. The third error is the zero draft. In order to remove the first error, the low-pass filter algorithm [53] is utilized to eliminate the high frequency noise. Fig. 1 shows the second error. We see that, the x , y and z axis in theory are completely orthogonal to each other in the ideal state. But in practice, acceleration measurement axis may not be in this ideal case. That is, the ideal conditions of the three-axis and the actual sensor do not entirely coincide. It is known as the sensor device error.

In order to eliminate second error, for each accelerometer sensor, we use the following linear fit equation to recover the accelerometer value a_{x_T} , a_{y_T} and a_{z_T} in the vector coordination (hardware coordinate) system

$$\begin{aligned} a_{x_T} &= k_x * a_x + b_x \\ a_{y_T} &= k_y * a_y + b_y \\ a_{z_T} &= k_z * a_z + b_z. \end{aligned} \quad (1)$$

In the above equation, a_{x_T} , a_{y_T} , a_{z_T} are the true value of the accelerometer along the x axis, y axis and z axis, respectively. a_x , a_y , a_z are the measured accelerometer data along the x , y and z axis, respectively. k_x and b_x , k_y and b_y , k_z and b_z are the correction factors of the accelerometer along the x , y and z axis, respectively, when the sensor stays static.

Taking the x axis as an example, we can use the least square method to determine the parameters k_x and b_x . In the above equation, a_{xti} is the real value, while a_{xi} is the measured value. In order to minimize the weighted average sum of the observed values, we only need to minimize the value of the following equation. Take partial derivatives of k_x and b_x of the above formula, then

$$\begin{aligned} &\frac{\partial}{\partial b_x} \sum_{i=1}^N [a_{xti} - (b_x + k_x a_{xi})]^2 \\ &= -2 \sum_{i=1}^N [a_{xti} - b_x - k_x a_{xi}] = 0 \end{aligned} \quad (2)$$

$$\begin{aligned} &\frac{\partial}{\partial k_x} \sum_{i=1}^N [a_{xti} - (b_x + k_x a_{xi})]^2 \\ &= -2 \sum_{i=1}^N [a_{xti} - b_x + (k_x a_{xi})] = 0. \end{aligned} \quad (3)$$

After finishing to

$$\begin{cases} b_x N + k_x \sum_{i=1}^N a_{xi} = \sum_{i=1}^N a_{xti} \\ b_x \sum_{i=1}^N a_{xi} + k_x \sum_{i=1}^N a_{xti}^2 = \sum_{i=1}^N a_{xti} a_{xi} \end{cases} \quad (4)$$

包括一个相机，IMU和EX传感器。此外，使用Kalman过滤器来稳定获得的姿势。这些技术需要部署各种设备，并且在实践中使用不便。

2.2 手势识别算法

有大量工作[44], [45], [46], [47], [48], [49], [50], [51]利用机器学习算法来识别人类手势。Zhu和Sheng [48]利用神经网络和隐藏的马尔可夫模型来认可手势。Zhao [49]提出了一种用于头部安装设备的实时手势系统。该系统主要训练收集的头部运动信息，以建立隐藏的马尔可夫模型，然后实时识别出ges。Wang and Chuang [46]利用线性分析分析(LDA)提取特征并采用概率神经网络(PNN)来识别手势。Wu和Sun [50]利用肌肉传感器和惯性传感器收集手语的手势数据，然后使用了支持向量机(SVM)，天真的贝叶斯(NB)和K-Neartimp邻居(KNN)算法对手势进行分类。Bhuyan [51]利用陀螺仪和加速度来预测臂的旋转方向，然后使用卡尔曼过滤器来查找手臂的确切位置。Wang等。[27]开发了拖曳生成的对抗网络(GAN)，即SS-GAN和St-Gan，以提高人类的识别精度。张等。[42]设计了一个电脑复发性神经网络(CRNN)结构，以识别手势。Gochoo等。[52]提出了一种采用深度卷积神经网络(DCNN)的基于IoT的隐私瑜伽姿势识别系统。

但是，这些机器学习算法只能识别在阶段训练的手势。如果发生了不同的手势，或者已经更换了目标人，或者甚至同一个人执行相同的态度，但幅度不同，这些方法可能无法识别它们。因此，机器学习算法只能识别有限数量的预定手势。特别是他们的培训成本很高。

在我们的工作中，即使手势相似，但幅度不同，我们也可以准确地识别出复杂的物质。与机器学习算法相比，我们的算法不需要高计算成本，并且可以在没有事先培训的情况下执行。

3 方法

在我们的方法中，我们首先消除了硬件设备的噪声和线性分解，然后消除了重力对此类数据的影响。在下文中，我们提出了一种综合算法，以实时跟踪人的手势，这可以消除硬件灵敏度差异，并有效利用身体运动的限制来显著提高跟踪精度。最后，我们提出了一种认可人体手势的认可算法。

3.1 陀螺仪降噪

陀螺仪传感器主要由三种错误组成。第一个错误是高频噪声。第二个错误是由焊接引起的硬件的线性失真

acy, plane curvature and roughness, as well as circuit

Authorized licensed use limited to: NANKAI UNIVERSITY. Downloaded on May 19, 2025 at 06:47:57 UTC from IEEE Xplore. Restrictions apply.

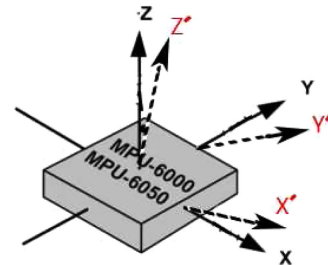


图1。硬件线性失真。X, Y和Z轴是理想的状态，而X', Y'和Z'是实际状态。

董事会会处理精度。第三个错误是零草稿。为了删除第一个误差，使用低通量过滤器算法[53]来消除高频噪声。图1显示了第二个错误。我们看到，在理想状态下，Ory中的X, Y和Z轴完全正交。但是实际上，在这种理想情况下，加速度测量轴可能不是。也就是说，三轴和实际传感器的理想条件并不完全重合。它被称为传感器设备误差。

为了消除第二个误差，对于每个加速度计传感器，我们使用以下线性拟合方程来恢复加速度计值 a_{x_T} , a_{y_T} 和向量协调(硬件坐标)系统中的 a_{z_T}

$$\begin{aligned} a_{x_T} &= k_x * a_x + b_x \\ a_{y_T} &= k_y * a_y + b_y \\ a_{z_T} &= k_z * a_z + b_z. \end{aligned} \quad (1)$$

在上面的方程式中， a_{x_T} , a_{y_T} , a_{z_T} 是沿x轴, y轴和z轴的加速度计的真实值。 a_x , a_y , a_z 分别是沿x, y和z轴的测量加速度计数据。 k_x 和 b_x , k_y 和 b_y , k_z 和 b_z 分别是沿X, Y和Z轴的加速度计的校正因子，当传感器保持静态时。

以X轴为例，我们可以使用最小平方的方法来确定参数 k_x 和 b_x 。在上面的方程式中， a_{x_T} 是实际值，而 a_x 是微音值。为了最大程度地减少观测值的加权平均值，我们只需要最大程度地减少下方程的值即可。采用上述公式的 k_x 和 b_x 的部分衍生物，然后

$$\begin{aligned} \frac{\partial}{\partial b_x} \sum_{i=1}^N [a_{xTi} - (b_x + k_x a_{xi})]^2 \\ = -2 \sum_{i=1}^N [a_{xTi} - b_x - k_x a_{xi}] = 0 \end{aligned} \quad (2)$$

$$\begin{aligned} \frac{\partial}{\partial k_x} \sum_{i=1}^N [a_{xTi} - (b_x + k_x a_{xi})]^2 \\ = -2 \sum_{i=1}^N [a_{xTi} - b_x + (k_x a_{xi})] = 0. \end{aligned} \quad (3)$$

填充后

$$\begin{cases} b_x N + k_x \sum_{i=1}^N a_{xi} = \sum_{i=1}^N a_{xTi} \\ b_x \sum_{i=1}^N a_{xi} + k_x \sum_{i=1}^N a_{xTi}^2 = \sum_{i=1}^N a_{xTi} a_{xi} \end{cases} \quad (4)$$

TABLE 1
Notations

Notation	Description
a_x, a_y, a_z	a_x, a_y and a_z respectively represent the acceleration data of x, y and z axis output by IMU inertial sensor.
g_x, g_y, g_z	g_x, g_y and g_z respectively represent the angular velocity data of x, y and z axis output by IMU inertial sensor.
C_w^w, C_b^b	C_w^w represents the transformation matrix from the carrier coordinate system to the world coordinate system, C_b^b represents the transformation matrix from the world coordinate system to the carrier coordinate system. They are inverse matrices.
(W_x, W_y, W_z)	(W_x, W_y, W_z) is the initial coordinate position of the sensor.
(W'_x, W'_y, W'_z)	(W'_x, W'_y, W'_z) is the initial coordinate position after the sensor is moved.
α, β, γ	α is the pitch around the x -axis. β is the yaw around the y -axis. γ is the roll angle around the z -axis.
$a_1, a_2, a_3, \dots, a_n$	$a_1, a_2, a_3, \dots, a_n$ refer to the received acceleration sequence, and a_i refers to the acceleration data received at time $i \times \Delta t$.
l	l represents the length of a part of the human body.

Solve the above equation to get

$$k_x = \frac{N \left(\sum_{i=1}^N a_{xi} a_{xti} \right) - \left(\sum_{i=1}^N a_{xi} \right) \left(\sum_{i=1}^N a_{xti} \right)}{N \left(\sum_{i=1}^N a_{xi}^2 \right) - \left(\sum_{i=1}^N a_{xi} \right)^2} \quad (5)$$

$$b_x = \frac{\left(\sum_{i=1}^N a_{xi}^2 \right) \left(\sum_{i=1}^N a_{xti} \right) - \left(\sum_{i=1}^N a_{xi} \right) \left(\sum_{i=1}^N a_{xi} a_{xti} \right)}{N \left(\sum_{i=1}^N a_{xi}^2 \right) - \left(\sum_{i=1}^N a_{xi} \right)^2}. \quad (6)$$

In the same way, we can also calculate the correction factors k_y, b_y and k_z, b_z of y axis and z axis respectively, so as to eliminate the influence of mechanical error on acceleration.

Zero drift [54] means that in the static situation, the output data is not equal to zero. Therefore, we use the difference between the actual measured value and the ideal value in the static case to replace the gyroscope data. g_x, g_y , and g_z are the actual data along x, y and z axis output by the gyroscope respectively, while g_{xt}, g_{yt} and g_{zt} are the data along x, y and z axis respectively in the ideal state, then

$$\begin{aligned} g_{xt} &= g_x + c_x \\ g_{yt} &= g_y + c_y \\ g_{zt} &= g_z + c_z. \end{aligned} \quad (7)$$

In the above formula, c_x, c_y and c_z are the static compensation quantities of x, y and z axes respectively. The sensor is placed in an arbitrary position, and the average value of q sets of gyroscope data of x, y and z axes are c_x, c_y and c_z , respectively. In this way, the gyroscope data of the MEMS sensor can be corrected.

Some important notations that will be used in this paper are listed in Table 1.

3.2 Noise Reduction of Acceleration Sensor

The data noise of the acceleration sensor mainly comes from two aspects. The first is the error caused by the mechanical imperfection of the hardware. The second is the influence of the acceleration due to gravity that always exists in space. To eliminate the first error, we use the linear distortion algorithm mentioned in the previous section. The second error is that g will have an impact on the z -axis of the world coordinate

system. However, the obtained sensor will transmit the sensing data based on the vector coordinate (hardware coordinate) system. Therefore, we should transform the acceleration data from the vector coordinate (hardware coordinate) system to the world coordinate system.

The gyroscope sensor describes how target object rotates. In Euler angle description, suppose ψ, θ and ϕ is the target rotation angle of z, y and x , representing Yaw, Pitch and Roll, respectively. According to [55], we can calculate the transformation matrix C_b^w from vector coordinate to world coordinate as shown below:

$$C_b^w = \begin{bmatrix} \cos \psi \cos \theta \cos \phi & \sin \psi \cos \theta & -\sin \theta \\ (\cos \psi \sin \theta \sin \phi - \sin \psi \sin \theta \sin \phi) & (\sin \psi \sin \theta \sin \phi + \cos \psi \sin \theta \sin \phi) & \cos \theta \sin \phi \\ (\cos \psi \sin \theta \cos \phi + \sin \psi \sin \theta \cos \phi) & (\sin \psi \sin \theta \cos \phi - \cos \psi \sin \theta \cos \phi) & \cos \theta \cos \phi \\ \sin \psi \sin \phi & \cos \psi \sin \phi & \cos \psi \sin \phi \end{bmatrix}. \quad (8)$$

Suppose in the hardware coordinate system, the acceleration data matrix from the accelerometer sensor is as follows:

$$a_w = [a_{wx} \ a_{wy} \ a_{wz}]^T. \quad (9)$$

In the absolute world coordinate system, the acceleration data can be expressed as shown below:

$$a_b = [C_b^w] \cdot [a_w] = [a_{bx} \ a_{by} \ a_{bz}]^T. \quad (10)$$

Since the impact of gravity affect only in the z axis of the world coordinate system, we only need to eliminate the g value along the z axis, that is

$$a_{bT} = [a_{bx} \ a_{by} \ a_{bz} - g]. \quad (11)$$

Hence, the impact of $|g|$ will be eliminated.

3.3 Tracking Algorithm of the Body Motion

After the previous pre-processing procedure, we utilize the following algorithm to track the body motion. Basically, our tracking algorithm consists of 4 sub-algorithms, which are performed along the sequence. First, a data noise elimination algorithm is proposed in Section 3.3.1. Second, we put forward a tracking algorithm for each wearable device in

表1符号

Notation	Description
a_x, a_y, a_z	a_x, a_y and a_z respectively represent the acceleration data of x, y and z axis output by IMU inertial sensor.
g_x, g_y, g_z	g_x, g_y and g_z respectively represent the angular velocity data of x, y and z axis output by IMU inertial sensor.
C_b^w, C_w^b	C_b^w represents the transformation matrix from the carrier coordinate system to the world coordinate system, C_w^b represents the transformation matrix from the world coordinate system to the carrier coordinate system. They are inverse matrices.
(W_x, W_y, W_z)	(W_x, W_y, W_z) is the initial coordinate position of the sensor.
(W'_x, W'_y, W'_z)	(W'_x, W'_y, W'_z) is the initial coordinate position after the sensor is moved.
α, β, γ	α is the pitch around the x -axis. β is the yaw around the y -axis. γ is the roll angle around the z -axis.
$a_1, a_2, a_3, \dots, a_n$	$a_1, a_2, a_3, \dots, a_n$ refer to the received acceleration sequence, and a_i refers to the acceleration data received at time $i \times \Delta t$.
l	l represents the length of a part of the human body.

解决上述方程式以获取

$$k_x = \frac{N \left(\sum_{i=1}^N a_{xi} a_{xti} \right) - \left(\sum_{i=1}^N a_{xi} \right) \left(\sum_{i=1}^N a_{xti} \right)}{N \left(\sum_{i=1}^N a_{xi}^2 \right) - \left(\sum_{i=1}^N a_{xi} \right)^2} \quad (5)$$

$$b_x = \frac{\left(\sum_{i=1}^N a_{xi}^2 \right) \left(\sum_{i=1}^N a_{xti} \right) - \left(\sum_{i=1}^N a_{xi} \right) \left(\sum_{i=1}^N a_{xi} a_{xti} \right)}{N \left(\sum_{i=1}^N a_{xi}^2 \right) - \left(\sum_{i=1}^N a_{xi} \right)^2}. \quad (6)$$

以同样的方式，我们还可以分别计算出Y轴和Z轴的校正 k_y , b_y 和 k_z , b_z ，以消除加速度机械误差的影响。

零漂移[54]意味着在静态情况下，外部数据不等于零。因此，我们使用静态情况下实际测量值和理想值之间的差异来替换陀螺仪数据。 g_x , g_y 和 g_z 分别是gyro-scope沿x, y和z轴沿x, y和z轴的实际数据，而 g_{xt} , g_{yt} , g_{zt} 分别沿x, y和z轴的数据分别是理想状态的数据

$$\begin{aligned} g_{xt} &= g_x + c_x \\ g_{yt} &= g_y + c_y \\ g_{zt} &= g_z + c_z. \end{aligned} \quad (7)$$

在上面的公式中， C_x , C_y 和 C_z 分别是X, Y和Z轴的静态组合量。传感器位于任意位置，X, Y和Z轴的陀螺仪数据的Q集的平均值分别为 C_x , C_y 和 C_z 。这样，可以纠正MEMS传感器的陀螺仪数据。

表1列出了本文中将使用的一些重要符号。

3.2 加速传感器的降噪

加速传感器的数据噪声主要来自两个方面。第一个是由硬件的机械缺陷造成的错误。第二个是由于重力而始终存在于太空中的加速度的影响。为了消除第一个错误，我们使用上一节中提到的线性失真算法。第二个错误是G将HA

系统。但是，获得的传感器将基于向量坐标（硬件坐标）系统传输感应数据。因此，我们应该将加速度数据从向量坐标（硬件坐标）系统转换为世界坐标系。

陀螺仪传感器描述了目标对象的旋转方式。在Euler角度描述中，假设C, U和F是Z, Y和X的目标旋转角，分别代表偏航，俯仰和滚动。根据[55]，我们可以计算从向量坐标到世界坐标的转换矩阵 C_b^w ，如下所示：

$$C_b^w = \begin{bmatrix} \cos \psi \cos \theta \cos \phi & \sin \psi \cos \theta & -\sin \theta \\ (\cos \psi \sin \theta \sin \phi - \sin \psi \sin \theta \sin \phi) & (\sin \psi \sin \theta \sin \phi + \cos \psi \sin \theta \sin \phi) & \cos \theta \sin \phi \\ (\cos \psi \sin \theta \cos \phi + \sin \psi \sin \theta \cos \phi) & (\sin \psi \sin \theta \cos \phi - \cos \psi \sin \theta \cos \phi) & \cos \theta \cos \phi \\ \sin \psi \sin \phi & \cos \psi \sin \phi & \cos \psi \sin \phi \end{bmatrix}. \quad (8)$$

假设在硬件坐标系中，加速度计传感器的加速数据矩阵如下：

$$a_w = [a_{wx} \ a_{wy} \ a_{wz}]^T. \quad (9)$$

在绝对世界坐标系中，加速度数据可以表示如下：

$$a_b = [C_b^w] \cdot [a_w] = [a_{bx} \ a_{by} \ a_{bz}]^T. \quad (10)$$

由于重力的影响仅在世界坐标系的Z轴上影响，因此我们只需要消除沿Z轴的G值，即

$$a_{b_T} = [a_{bx} \ a_{by} \ a_{bz} - g]. \quad (11)$$

因此，将消除JGJ的影响。

3.3 跟踪身体运动的算法

在先前的预处理程序之后，我们利用以下算法来跟踪身体运动。基本上，我们的跟踪算法由4个沿序列执行的4个子算法组成。首先，在第3.3.1节中提出了数据噪声消除算法。其次，我们放了

Section 3.3.2. Such algorithm is able to calculate the coordinates of each device. These coordinates will form a trace of such device. Third, we use a hardware difference elimination algorithm to refine the tracking accuracy in Section 3.3.3. At last, we leverage the correlation and limitation among body parts to optimize the tracking accuracy in Section 3.3.4.

3.3.1 Elimination of Data Noise

Suppose each sensor will transmit its acceleration data every time interval Δt , and n is the total number of transmitted packets, we may obtain acceleration data array a_n in theory. In practice, if a_i ($1 < i < n$) is not received by the receiver, we need to insert an interpolation value in the array as follows:

$$a_i = (a_{i+1} + a_{i-1})/2. \quad (12)$$

In particular, when successive values are not received, we use the following formula to insert values:

$$a_{k_j} = \frac{a_{end} - a_{start}}{k+1} * j + a_{start}. \quad (13)$$

In the above formula, a_{k_j} means that the j th value in the k continuously missing values. a_{start} and a_{end} represents the first and the last of the continuously missing values respectively.

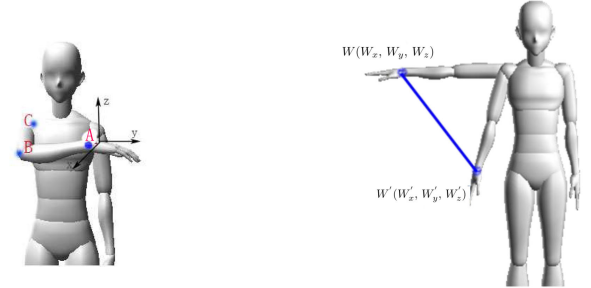
In the following, we utilize the five-spot triple smoothing method [56] to reduce the high frequency random noise. Suppose there are n number of received acceleration data represented by a data array a_n , within a sampling time interval Δt , and let $a_{i-2}, a_{i-1}, a_i, a_{i+1}$ and a_{i+2} be any five continuous received acceleration data, they can be used to recalculated as follows:

$$\begin{aligned} \bar{a}_{i-2} &= \frac{1}{70}(69a_{i-2} + 4a_{i-1} - 6a_i + 46a_{i+1} - a_{i+2}) \\ \bar{a}_{i-1} &= \frac{1}{35}(2a_{i-2} + 27a_{i-1} + 12a_i - 8a_{i+1} + 2a_{i+2}) \\ \bar{a}_i &= \frac{1}{35}(-3a_{i-2} + 12a_{i-1} + 17a_i + 12a_{i+1} - 3a_{i+2}) \\ \bar{a}_{i+1} &= \frac{1}{35}(2a_{i-2} - 8a_{i-1} + 12a_i + 27a_{i+1} + 2a_{i+2}) \\ \bar{a}_{i+2} &= \frac{1}{70}(-a_{i-2} + 4a_{i-1} - 4a_i + 4a_{i+1} + 69a_{i+2}). \end{aligned} \quad (14)$$

In the above formula, $\bar{a}_{i-2}, \bar{a}_{i-1}, \bar{a}_i, \bar{a}_{i+1}, \bar{a}_{i+2}$ means the refine result respectively. The coefficients in the equations are refined by [56]. The initial a_0 and a_1 may be estimated from the first and second equation. The final a_{n-1} and a_n may be recalculated from the fourth and fifth equation. Other a_i can be derived from the third equation.

3.3.2 Basic Motion Tracking Algorithm for Each Wearable Device

In the previous subsections, we have already finished refining the hardware linear distortion, eliminating the impact of gravity and noise. Therefore, in this subsection, we may utilize the processed acceleration data to accurately calculate the displacement of each wearable device and derive the gesture in real time.



(a) Deployment example. The 3 wearable sensors A, B, C are put on the human wrist, elbow and shoulder, respectively.

(b) The displacement.

Fig. 2. (a) Deployment example. The 3 wearable sensors A, B, C are put on the human wrist, elbow and shoulder, respectively. (b) The displacement.

In our first attempt, we leverage simpson double integral [57] to calculate the displacement of each wearable device as follows:

$$\begin{aligned} v_i &= v_{i-1} + ((a_{i-1} + 4a_i + a_{i+1})/6) \cdot \Delta t \\ s_i &= s_{i-1} + ((v_{i-1} + 4v_i + v_{i+1})/6) \cdot \Delta t, \end{aligned} \quad (15)$$

where v_i is the velocity of the target sensor at time t_i ($i \in (1, n)$, n is the number of received acceleration data), s_i is the total accumulate displacement of the target sensor at time t_i , Δt is the time interval of sampling. s_n is the total displacement after receiving n number of acceleration data.

In our work, the sensors are placed on the joints of the human body. Suppose that a certain fixed point of the body is the origin, then according to the relationship between the human joints, we can get the initial coordinates of the sensor at other joints. As shown in Fig. 2b, assume that there is a wearable sensing device W , let its initial coordinate be $W(W_x, W_y, W_z)$, then the coordinate of such device after moving is expressed as $W'(W'_x, W'_y, W'_z)$, which can be further expressed as

$$\begin{aligned} W'_x &= W_x + s_{nx} \\ W'_y &= W_y + s_{ny} \\ W'_z &= W_z + s_{nz}, \end{aligned} \quad (16)$$

where s_{nx}, s_{ny} and s_{nz} are the integration results s_n mapping to x, y and z axis, respectively.

3.3.3 Improvement Method 1: Eliminate Hardware Difference on Tracking Accuracy

There are sensing variance among different wearable sensor devices. Even for the same sensor, the sensitivity of accelerometer along x, y and z axis are also different. Therefore, in order to eliminate such difference, for each sensing device, we calculate a correction factor u_p and u_n for the positive direction and negative direction along each axis. Taking the x axis as an example, u_{xp} and u_{xn} are the results u_p and u_n mapping to position and negative direction of x axis, respectively. It can be represented by the following equation:

$$\begin{aligned} u_{xp} &= (d_{cpx} - d_{rpx})/d_{rpx} \\ u_{xn} &= (d_{cxn} - d_{rxn})/d_{rxn}, \end{aligned} \quad (17)$$

第3.3.2节。这种算法能够计算每个设备的坐标。这些坐标将形成这种设备的轨迹。第三，我们使用硬件差消除算法来确定第3.3.3节中的跟踪精度。最后，我们利用身体部位之间的相关性和限制来优化第3.3.4节中的跟踪准确性。

3.3.1 消除数据噪声

假设每个传感器将每个时间间隔 Δt 传输其加速度数据，而n是传输数据包的总数，我们可以从理论上获得加速度数据阵列 a_n 。实际上，如果接收器未收到 i ($1 < i < n$)，我们需要在数组中插入一个插值值，如下所示：

$$a_i = (a_{i+1} + a_{i-1})/2. \quad (12)$$

特别是，当未收到连续值时，我们使用以下公式插入值：

$$a_{kj} = \frac{a_{end} - a_{start}}{k+1} * j + a_{start}. \quad (13)$$

在上面的公式中， a_{kj} 表示k中的jth值连续丢失值。 a_{start} 和 a_{end} 分别代表连续缺失的值的第一个和最后一个。

在下文中，我们利用五个点三重平滑法[56]来减少高频随机噪声。Suppose there are n number of received acceleration data represented by a data array a_n , within a sampling time interval Δt , and let $a_{i-2}, a_{i-1}, a_i, a_{i+1}$ and a_{i+2} be any five continuous received acceleration data, they can be used to recalculated as follows:

$$\begin{aligned} \bar{a}_{i-2} &= \frac{1}{70}(69a_{i-2} + 4a_{i-1} - 6a_i + 46a_{i+1} - a_{i+2}) \\ \bar{a}_{i-1} &= \frac{1}{35}(2a_{i-2} + 27a_{i-1} + 12a_i - 8a_{i+1} + 2a_{i+2}) \\ \bar{a}_i &= \frac{1}{35}(-3a_{i-2} + 12a_{i-1} + 17a_i + 12a_{i+1} - 3a_{i+2}) \\ \bar{a}_{i+1} &= \frac{1}{35}(2a_{i-2} - 8a_{i-1} + 12a_i + 27a_{i+1} + 2a_{i+2}) \\ \bar{a}_{i+2} &= \frac{1}{70}(-a_{i-2} + 4a_{i-1} - 4a_i + 4a_{i+1} + 69a_{i+2}). \end{aligned} \quad (14)$$

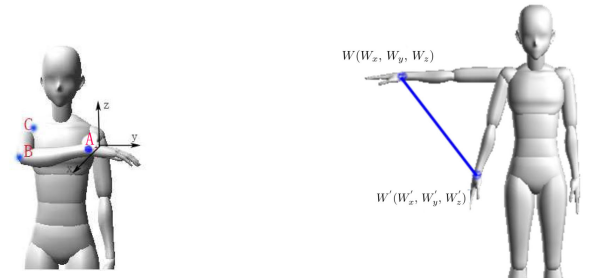
在上面的公式中， $\bar{a}_{i-2}, \bar{a}_{i-1}, \bar{a}_i, \bar{a}_{i+1}, \bar{a}_{i+2}$ 分别表示重新效果。方程中的系数由[56]重新填充。可以从第一个和第二个方程式估算初始 A_0 和 A_1 。最终 A_{n-1} 和 A_n 可以从第四和第五方程重新计算。其他 A_i 可以从第三个方程得出。

3.3.2 每个可穿戴设备的基本运动跟踪算法

在先前的小节中，我们已经完成了硬件线性失真的结构，从而消除了重力和噪声的影响。因此，在本小节中，我们可以利用处理后的加速度数据来准确计算每个可穿戴设备的位移，并得出 g_{est}

ure in real time.

Authorized licensed use limited to: NANKAI UNIVERSITY. Downloaded on May 19, 2025 at 06:47:57 UTC from IEEE Xplore. Restrictions apply.



(a) Deployment example. The 3 wearable sensors A, B, C are put on the human wrist, elbow and shoulder, respectively.

(b) The displacement.

图2。 (a) 部署示例。3个可穿戴传感器A, B, C分别放在人的手腕,肘部和肩膀上。 (b) 位移。

在我们的第一次尝试中，我们利用Simpson Double Integrals [57]来计算每个可穿戴设备的位移，如下所示：

$$\begin{aligned} v_i &= v_{i-1} + ((a_{i-1} + 4a_i + a_{i+1})/6) \cdot \Delta t \\ s_i &= s_{i-1} + ((v_{i-1} + 4v_i + v_{i+1})/6) \cdot \Delta t, \end{aligned} \quad (15)$$

其中 v_i 是时间 t_i ($i \geq 1$ 时目标传感器的速度；n, n是接收到的加速度数据)， s_i 是目标传感器在时间 t_i ， Δt 的总累加位移是采样的时间间隔。 S_n 是接收N加速度数据数量后的总位移。

在我们的工作中，传感器放在人体的关节上。假设身体的某个固定点是起源，然后根据人关节之间的关系，我们可以在其他关节处获得传感器的初始坐标。如图2b所示，假设有一个可穿戴的传感设备W，让其初始坐标为 $w(\omega_x, \omega_y, \omega_z)$ ，然后移动后这种设备的坐标表示为 $w'(\omega'_x, \omega'_y, \omega'_z)$ ，f {

$$\begin{aligned} \omega'_x &= \omega_x + s_{nx} \\ \omega'_y &= \omega_y + s_{ny} \\ \omega'_z &= \omega_z + s_{nz}, \end{aligned} \quad (16)$$

其中 s_{nx}, s_{ny} 和 s_{nz} 分别是集成结果 s_n 映射到x, y和z轴。

3.3.3 改进方法1：消除跟踪精度的硬件差异

不同的可穿戴传感器设备之间有传感差异。即使对于同一传感器，沿X, Y和Z轴的加速度的灵敏度也不同。因此，为了消除这种差异，对于每个感应设备，我们计算一个校正因子 u_p 和 u_n ，沿每个轴的正方向和负方向。以X轴为例， U_{xp} 和 U_{xn} 是结果 U_p 和 U_n 映射到X轴的位置和负方向，从而分配。它可以用以下等式表示：

$$\begin{aligned} u_{xp} &= (d_{cgp} - d_{rnp})/d_{rnp} \\ u_{xn} &= (d_{cxn} - d_{rxn})/d_{rxn}, \end{aligned} \quad (17)$$

where d_r represents the real displacement of the wearable sensing device. d_r is obtained by manual measurement. d_c is the calculated displacement by the basic tracking algorithm introduced in the last subsection. In real application, we may perform a number of tests (e.g., 10), and utilize the average calculated displacement to represent d_c . d_{rxp} and d_{cxp} are d_r and d_c mapping to positive direction of x axis. d_{rnx} and d_{cnx} are d_r and d_c mapping to the negative direction of x axis.

Therefore, the displacement of x axis can be refined by u_{xp} and u_{xn} as follows:

$$\begin{aligned} s_{uxp} &= s_{nxp}/(1 + u_{xp}) \\ s_{uxn} &= s_{nxn}/(1 + u_{xn}), \end{aligned} \quad (18)$$

here s_{nxp} and s_{nxn} are mapping to the positive direction calculated displacement and negative direction calculated displacement of s_{nx} , respectively. Assume that there is a wearable sensing device M , its initial coordinate is $M(M_x, M_y, M_z)$, then the coordinate of such device after being refined by correction factor is expressed as $M'(M'_x, M'_y, M'_z)$, the x coordinate can be expressed as

$$M'_x = M_x + s_{ux}, \quad (19)$$

here s_{ux} value determined by the following formula:

$$s_{ux} = \begin{cases} s_{uxp} & s_{nx} > 0 \\ s_{uxn} & s_{nx} \leq 0 \end{cases} \quad (20)$$

The correction factors of the other axis are calculated following the same rule.

3.3.4 Improvement Method 2: Enhance the Tracking Accuracy by Using the Correlation and Limitation Among Body Parts

Since each wearable device is fixed on a certain position of the human body, its moving trajectory will be in accordance with the common human motion. Therefore, we can take advantage of this correlation and limitation among body parts to optimize the tracking results.

We use the following criteria to determine whether to use the improvement method

$$M_{distance} = \sqrt{(M_x - M'_x)^2 + (M_y - M'_y)^2 + (M_z - M'_z)^2} \quad (21)$$

$$G_i = \begin{cases} G_{small} & M_{distance} > l \\ G_{large} & M_{distance} \leq l \end{cases} \quad (22)$$

In the above criteria, l is a threshold, which can be defined according to the user requirements (in our experiment, we set the value of l as half of the largest gesture amplitude which can be performed by human body). We calculate the displacement of the gesture, when the displacement is larger than l , we define it as a large amplitude gesture G_{large} , otherwise we define it as a small amplitude gestures G_{small} .

In the example shown in Fig. 2a, the 3 wearable sensors A , B , C are put on the human wrist, elbow and shoulder, respectively. Since the lengths of the human upper arm and

lower arm are both fixed, the distance between A and B , B and C are also fixed. In such example, we may refine the tracking error as follows. Let the length of the human upper arm is r_1 (the distance between A and B), and the human lower arm is r_2 (the distance between B and C). Since in this example, the shoulder is fixed, let its initial coordinate be (C_x, C_y, C_z) . The calculated coordinate of point A' by improvement method 1 is (A'_x, A'_y, A'_z) . The calculated coordinate of point B' by improvement method 1 is (B'_x, B'_y, B'_z) . The final calculated coordinate $B_F(B_{Fx}, B_{Fy}, B_{Fz})$ for node B' is

$$\begin{aligned} B_{Fx} &= B'_x + (r_1 * (B'_x - C_x))/d_{B'C} \\ B_{Fy} &= B'_y + (r_1 * (B'_y - C_y))/d_{B'C} \\ B_{Fz} &= B'_z + (r_1 * (B'_z - C_z))/d_{B'C} \\ d_{B'C} &= \sqrt{(B'_x - C_x)^2 + (B'_y - C_y)^2 + (B'_z - C_z)^2}. \end{aligned} \quad (23)$$

The final calculated coordinate $A_F(A_{Fx}, A_{Fy}, A_{Fz})$ for node A' is

$$\begin{aligned} A_{Fx} &= A'_x + (r_2 * (A'_x - B_{Fx}))/d_{A'B'} \\ A_{Fy} &= A'_y + (r_2 * (A'_y - B_{Fy}))/d_{A'B'} \\ A_{Fz} &= A'_z + (r_2 * (A'_z - B_{Fz}))/d_{A'B'} \\ d_{A'B'} &= \sqrt{(A'_x - B_{Fx})^2 + (A'_y - B_{Fy})^2 + (A'_z - B_{Fz})^2}. \end{aligned} \quad (24)$$

In the above equation, $d_{B'C}$ and $d_{A'B'}$ respectively denote the distance between point C and point B' , and the distance between point B' and point A' .

Since we can trace the trajectory of the sensors and the sensors are placed on the joints of the human body, combining with the correlation among the joints of the human body, we can precisely recognize the human gestures.

3.4 Recognition Algorithm

After obtaining the coordinates of each sensor placed on the human joints, we can recognize the human gesture by comprehensively considering the whole information. Suppose a person wears n sensors on the body, each sensor has displacement data along x , y and z axes, then each data of gesture is a $3 * n$ vector.

As shown in Fig. 3, assuming that D is our gesture library and there are a total of m gestures in D , then D is a $3 * n * m$ dimensional matrix, and we can use the following formula to identify gestures:

$$i^* = \operatorname{argmin} \|Ge - D_i\|_2^2, i = 1, \dots, n. \quad (25)$$

In the above formula, Ge represents the gesture vector to be recognized, and D_i represents the i gesture in the gesture library D . Finding an i^* which minimizes the formula, we can regard D_{i^*} as the gesture of Ge .

4 EXPERIMENT

In this section, we first introduce our implementation, followed by the investigation of key factors. At last, our motion tracking results in real time are given.

其中 d_r 表示可穿戴感应设备的真实位移。 D_r 是通过手动测量获得的。 D_c 是通过最后一个小节中引入的基本跟踪算法计算出的位移。在实际应用中，我们可以执行许多测试（例如10），并利用平均计算的位移来表示 D_{co} 。 d_{rxp} 和 d_{cxp} 是 d_r 和 d_c 映射到x轴的正方向。 d_{rxn} 和 d_{cxn} 是 d_r 和 d_c 映射到x轴的负方向。

因此，X轴的位移可以通过 U_{xp} 和 U_{xn} 进行重新填充，如下所示：

$$\begin{aligned} s_{uxp} &= s_{nxp}/(1 + u_{xp}) \\ s_{uxn} &= s_{nxn}/(1 + u_{xn}), \end{aligned} \quad (18)$$

这里的 s_{nxp} 和 s_{nxn} 分别映射到正方向计算的位移和负方向分别计算出 s_{nx} 的位移。假设有一个可穿戴的传感设备M，其初始坐标为 $m\delta m_x, m_y, m_z$ ，然后通过校正因子对此设备的坐标表示为 $m' \delta m'_x, m'_y, m'_z, v23\}$ ， $m \{$

$$M'_x = M_x + s_{ux}, \quad (19)$$

在这里 s_{ux} 值由以下公式确定：

$$s_{ux} = \begin{cases} s_{uxp} & s_{nx} > 0 \\ s_{uxn} & s_{nx} \leq 0 \end{cases} \quad (20)$$

在同一规则的情况下计算了其他轴的校正因子。

3.3.4 改进方法2：通过使用身体部位之间的相关性和限制来提高跟踪精度

由于每个可穿戴设备都在人体的某个位置上固定，因此其移动轨迹将与普通的人类运动相符。因此，我们可以利用身体部位之间的这种相关性和限制来优化跟踪结果。

我们使用以下标准来确定是否使用改进方法

$$M_{distance} = \sqrt{(M_x - M'_x)^2 + (M_y - M'_y)^2 + (M_z - M'_z)^2} \quad (21)$$

$$G_i = \begin{cases} G_{small} & M_{distance} > l \\ G_{large} & M_{distance} \leq l \end{cases} \quad (22)$$

在上述标准中，L是一个阈值，可以根据用户要求来定义（在我们的经验中，我们将L的值设置为可以由人体执行的最大手势振幅的一半）。我们计算手势的位移，当分位数大于L时，我们将其定义为大幅度手势 g_{large} ，否则我们将其定义为小振幅手势 g_{small} 。

在图2a所示的示例中，将3个可穿戴传感器A，B，C放在人的腕部，肘部和肩膀上，尊重

ively. Since the lengths of the human upper arm and
Authorized licensed use limited to: NANKAI UNIVERSITY. Downloaded on May 19, 2025 at 06:47:57 UTC from IEEE Xplore. Restrictions apply.

下臂均固定，A和B，B和C之间的距离也被固定。在这样的示例中，我们可以按以下方式重新填充跟踪误差。令人的上臂的长度为 r_1 （a和b）之间的距离，而人的下臂为 r_2 （b和c）之间的距离。由于在此示例中，将肩膀固定，因此让其初始坐标为 (c_x, c_y, c_z) 。通过改进方法1的点A'的计算坐标为 $\delta a'_x, a'_y, a'_z$ 。通过改进方法1的点B'计算出的坐标为 $\delta b'_x, b'_y, b'_z$ 。最终计算的坐标 $b_F \delta b_{Fx}, b_F y, b_F z$ 为节点b'是

$$\begin{aligned} B_{Fx} &= B'_x + (r_1 * (B'_x - C_x)) / d_{B'C} \\ B_{Fy} &= B'_y + (r_1 * (B'_y - C_y)) / d_{B'C} \\ B_{Fz} &= B'_z + (r_1 * (B'_z - C_z)) / d_{B'C} \\ d_{B'C} &= \sqrt{(B'_x - C_x)^2 + (B'_y - C_y)^2 + (B'_z - C_z)^2}. \end{aligned} \quad (23)$$

最终计算的坐标 $a_F \delta a_{Fx}, a_F y, a_F z$ 为节点a'是

$$\begin{aligned} A_{Fx} &= A'_x + (r_2 * (A'_x - B_{Fx})) / d_{A'B'} \\ A_{Fy} &= A'_y + (r_2 * (A'_y - B_{Fy})) / d_{A'B'} \\ A_{Fz} &= A'_z + (r_2 * (A'_z - B_{Fz})) / d_{A'B'} \\ d_{A'B'} &= \sqrt{(A'_x - B_{Fx})^2 + (A'_y - B_{Fy})^2 + (A'_z - B_{Fz})^2}. \end{aligned} \quad (24)$$

在上面的方程式中， $d_{B'C}$ 和 $d_{A'B'}$ 分别表示点C和点B'之间的距离，以及点B'和点A'之间的距离。

由于我们可以追踪传感器的轨迹，并将传感器放置在人体的关节上，并结合人体关节之间的相关性，因此我们可以精确地识别人类的手势。

3.4 识别算法

在获得了放置在人类关节上的每个传感器的坐标之后，我们可以通过预知考虑整个信息来识别人类的手势。假设一个人在体内戴上N传感器，每个传感器都有沿X，Y和Z轴的偏置数据，然后GESTURE的每个数据都是 $3 * n$ 向量。

如图3所示，假设D是我们的手势库，并且D中有大量的手势，那么D是 $3 * n * m$ 维矩阵，我们可以使用以下公式来识别手势：

$$i^* = argmin \|Ge - D_i\|_2^2, i = 1, \dots, n. \quad (25)$$

在上面的公式中，GE代表要识别的手势向量，而 D_i 表示手势库中的i手势D。找到最小化公式的 i^* ，我们可以将 D_{i^*} 视为GE的手势。

4实验

在本节中，我们首先介绍了我们的实施，这是对关键因素的调查。最后，我们的动作

tracking results in real time are given.

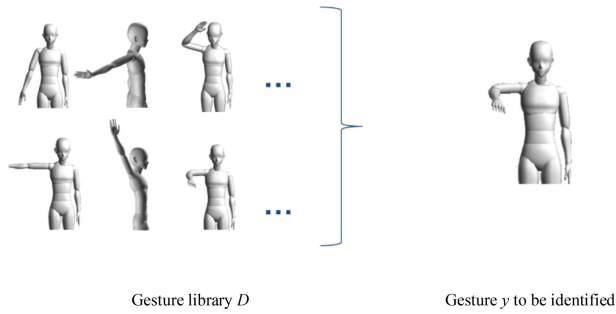


Fig. 3. Gesture library.

4.1 Implementation

In our experiment, we utilize the mpu6050 sensors. Each sensor contains a MEMS 3-axis accelerometer and a MEMS 3-axis gyro in a single chip. The low-pass filter algorithm is also integrated in the chips. The cutoff frequency is set as 44 Hz, since such setting will have both low latency and high filtering effect according to mpu6050 manual [58]. The communication module is nrf51822. Its core is ARM Cortex-M0. Keil is our programming and debugging tool. The part of the implementation code of the algorithm is in <https://github.com/630440348/Fine-grained-and-Real-time-Gesture-Recognition>.

Our framework chart is described in Fig. 4. We can divide the whole system into three parts: data preprocessing, displacement calculation and classification of gesture. In the first data preprocessing, we process the data collected from sensors and correct the hardware errors. In the following, we use a series of noise reduction method mentioned in the previous section to eliminate error. In particular, when data is missing, we also provide methods to supplement the missing value, as shown in Formulas (12), (13), and (14). In the second part, we use our recognition algorithms to calculate the displacement of the gesture movement mentioned

in Section 3. At last in the part of classification of gesture, by using our gesture recognition algorithm, we are able to output the gesture and the gesture type.

Before running our algorithm, the sensors are put on the fixed positions of the human body. Each sensor will transmit its sensing data back to the server by using Bluetooth protocol [59]. The transmission time interval of each sensor is set as 10 ms. The recognition algorithm is run on the server. For each sensor, when the total number of received packets reaches 80, the location of such sensor will be calculated. Such procedure is repeated, and the trajectory of each sensor will be obtained.

4.2 Results of Refining Hardware Linear Distortion and Eliminating Gravity Impact

In this subsection, we randomly chose a sensor and test it in stationary state. Before running our algorithm, the obtained accelerometer data are shown in Fig. 5a. We see that, the acceleration data along the x and y axis are not equal to 0(m/s^2) (due to the hardware linear distortion). Even worse, the acceleration data along the z axis are about 10(m/s^2) (due to the impact of the gravity). After using our algorithm, the results are shown in Fig. 5b. We may see that, both the hardware linear distortion of each axis and the impact of gravity are successfully eliminated. The acceleration data of each axis are all close to 0(m/s^2) in stationary status.

4.3 Noise Reduction

In this subsection, we will investigate the impact of the five-spot triple smoothing method. As Shown in Fig. 6, we utilized the smoothing method to deal with the acceleration signal. The top sub figure is the original acceleration signal before processing. The bottom sub figure is the result after smoothing. According to the figure, we can see that, the five-spot triple smoothing method can reduce the high

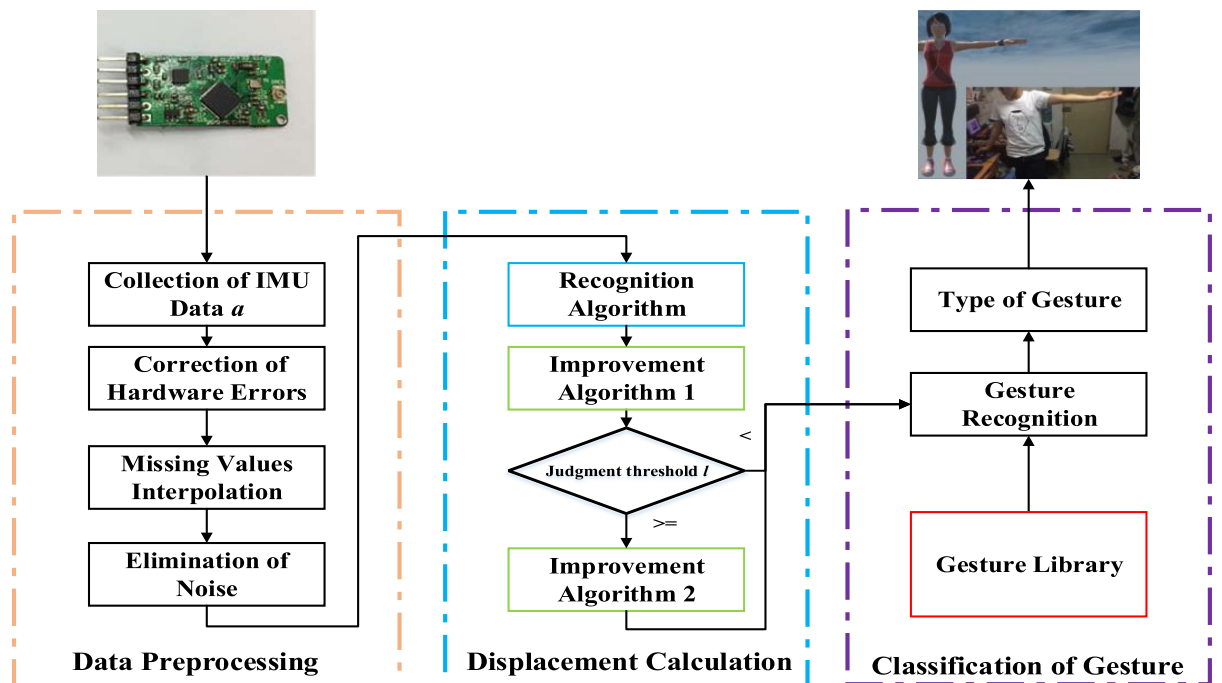


Fig. 4. Framework.

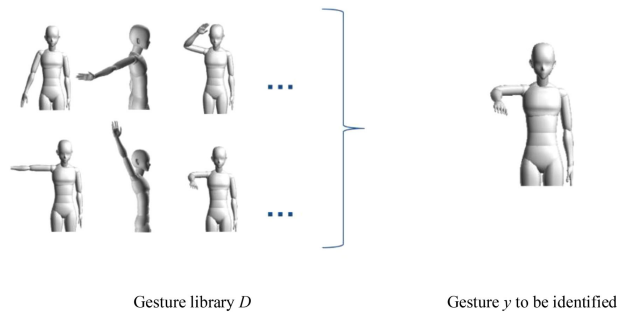


图3。手势库。

4.1实施

在我们的实验中，我们使用MPU6050传感器。每个传感器都包含一个MEMS 3轴加速度计和单个芯片中的MEMS 3轴陀螺仪。低通量过滤器算法也集成在芯片中。截止频率设置为44 Hz，因为根据MPU6050手册[58]，这种设置将具有较低的延迟和高过滤效果。通信模块是NRF51822。它的核心是ARM Cortex-M0。Keil是我们的编程和调试工具。该算法的实现代码的一部分在<https://github.com/630440348/罚款且实用的时间识别>中。

我们的框架图表如图4所述。我们可以将整个系统分为三个部分：手势的数据预处理，位移计算和分类。在第一个数据预处理中，我们处理从传感器收集的数据并纠正硬件错误。在下面，我们使用上一节中提到的一系列降低方法来消除误差。特别是，当缺少数据时，我们还提供了补充缺失值的方法，如公式 (12), (13) 和 (14) 中所示。在第二部分中，我们使用识别算法来计算提到的手势运动的位移

在第3节中。最后，在手势分类的一部分中，通过使用我们的手势识别算法，我们能够超越手势和手势类型。

在运行我们的算法之前，传感器被放在人体的固定位置上。每个传感器将使用蓝牙协议[59]将其传感数据传输回服务器。每个传感器的传输时间间隔设置为10 ms。识别算法在服务器上运行。对于每个传感器，当接收到的数据包的总数达到80时，将计算此类传感器的位置。重复此类过程，并获得每个传感器的轨迹。

4.2重新发现硬件线性失真并消除重力影响的结果

在本小节中，我们随机选择一个传感器并以固定状态进行测试。在运行我们的算法之前，获得的加速度计数据如图5A所示。我们看到，沿x和y轴的加速度数据不等于 $0\delta m/s^2$ （由于硬件线性失真）。更糟糕的是，沿Z轴的加速度数据约为 $1\delta m/s^2$ （由于重力的影响）。使用我们的算法后，结果如图5B所示。我们可能会看到，每个轴的硬件线性失真和重力的影响都被成功消除。每个轴的加速度数据都接近 $0\delta m/s^2$ s固定状态。

4.3降噪

在本小节中，我们将研究五个三重平滑法的影响。如图6所示，我们介绍了处理加速信号的平滑方法。顶部的最高子形是处理前的原始加速信号。底部子图是平滑后的结果。根据图，我们可以看到，五个点三重平滑方法可以降低高

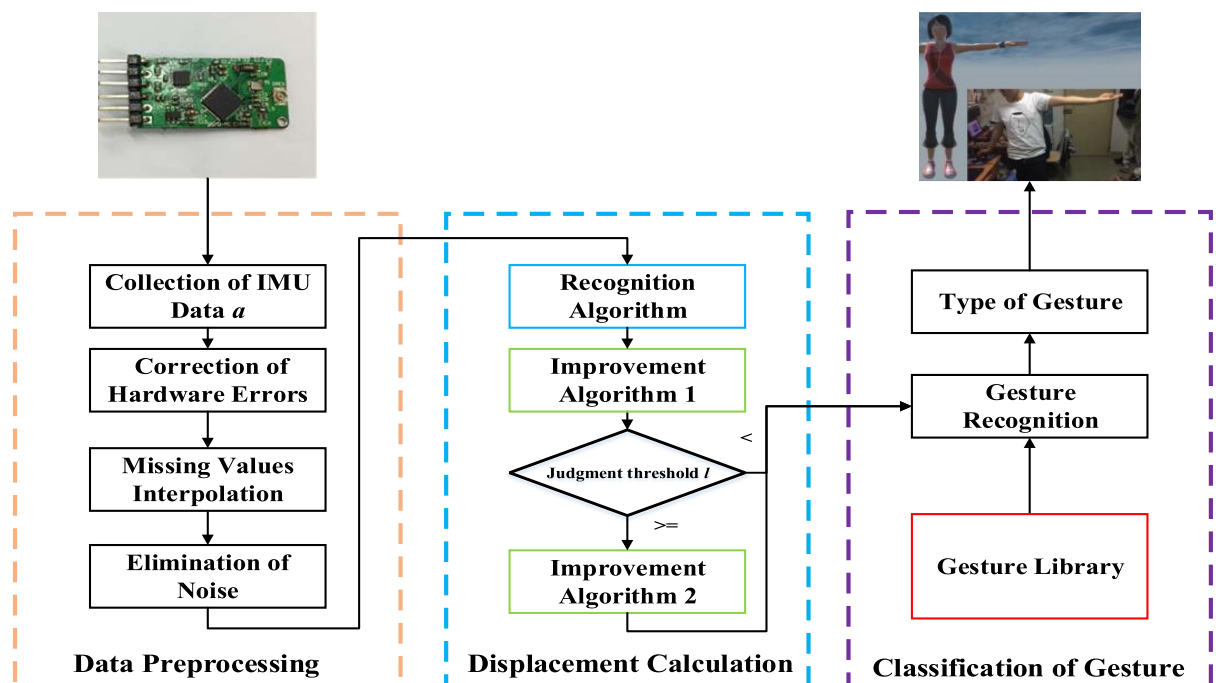


图4。框架。

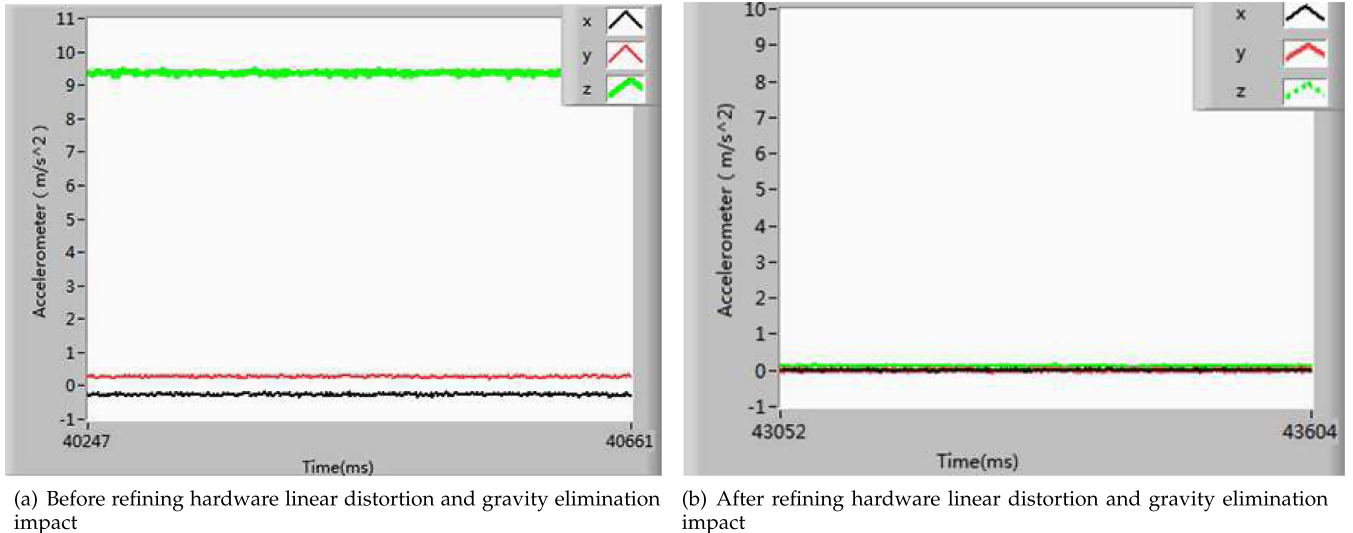


Fig. 5. Data correction of gyroscope and accelerometer.

frequency random noise in the signal, which can help later displacement calculation.

4.4 Accuracy of the Gesture Recognition

In this subsection, we will test how our algorithm will be able to successfully track human gesture.

In our experiments, the sensors were placed on the arm. In total, we tested 40 sets of gestures by 10 people with different height and weight. The height of the target varies from 150 cm to 182 cm, while the weight of the target varies from 45 kg to 80 kg. The tested gestures are shown in Fig. 7. Our gestures include waving arms, lifting arms, dropping arms, etc. The moving range description of the tested gestures is shown in Table 2. We can see the minimum and maximum degree of the roll, pitch and yaw. The maximum and minimum displacement of the tested gestures are 10 cm and 150 cm, respectively.

Fig. 8 shows the Cumulative Density Function (CDF) of accuracy, which is the difference between the calculated displacement and the real displacement. Our experiment results show that, our approach is able to successfully recognize the human gestures. We calculate the successful recognition rate

as the number of successful recognition times over the number of whole tested gestures. How to identify the gesture is calculated by Equation (25). Experimental results show that the successful recognition rate can reach 100%. The experiment results are shown in Figs. 8a and 8d. We can see that, the average accuracy is about 0.07 m. By using the improvement methods 1 and 2, the average accuracy can reach about 0.06 m. Hence, the average accuracy can be improved by about 15%.

In order to investigate which improvement method contributes the most, we tested 20 rounds of gestures with large amplitude, and another 20 rounds of gestures with small amplitude, respectively. The experiment results are shown in Figs. 8b and 8e and Figs. 8c and 8f. We find that, for the gestures with large amplitude, the tracking accuracy is best when both the improvement methods are used. While for the gestures with small amplitude, improvement method 1 is the best. The reason for this is the following. For the improvement method 2, we use the correlation and limitation among

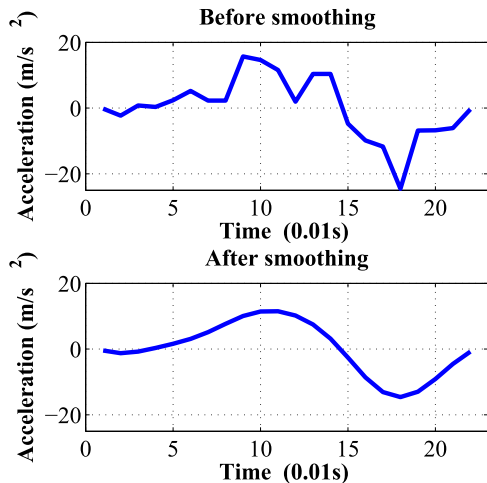


Fig. 6. Before and after smoothing.

Authorized licensed use limited to: NANKAI UNIVERSITY. Downloaded on May 19, 2025 at 06:47:57 UTC from IEEE Xplore. Restrictions apply.

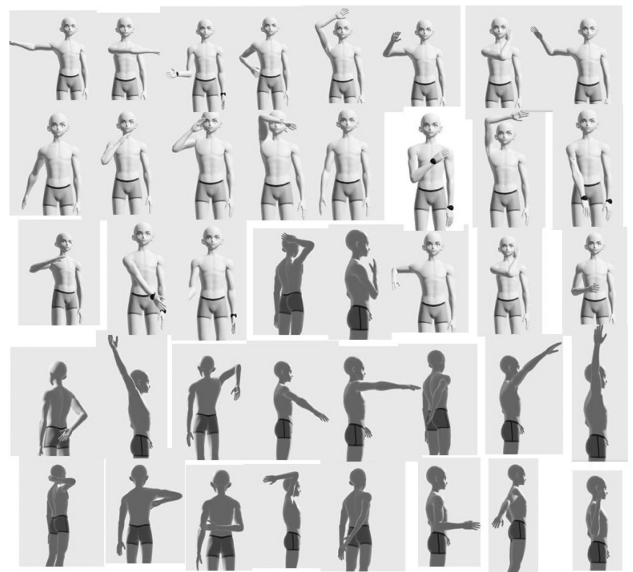
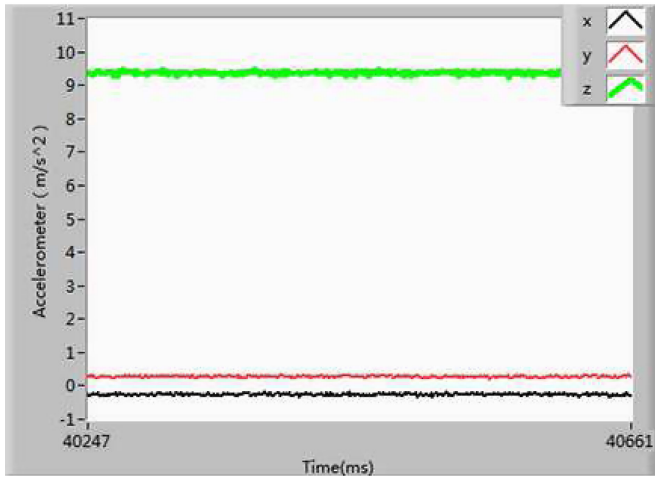
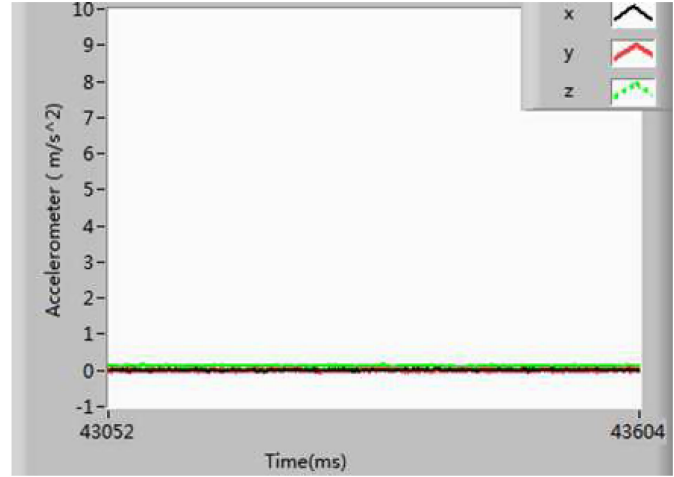


Fig. 7. The tested 40 gestures.



(a) Before refining hardware linear distortion and gravity elimination impact



(b) After refining hardware linear distortion and gravity elimination impact

图5。陀螺仪和加速度计的数据校正。

信号中的频率随机噪声可以帮助以后的位移计算。

4.4 手势识别的准确性

在本小节中，我们将测试我们的算法如何成功跟踪人类的手势。

在我们的实验中，将传感器放在手臂上。我们总共测试了40套手势，有10人的身高和体重不同。目标高度从150厘米到182厘米不等，而目标的重量从45千克到80千克不等。测试的手势如图7所示。我们的手势包括挥舞着手臂，抬起手臂，掉落的手臂等。表2中显示了测试的镜头的移动范围描述。我们可以看到滚动，螺距和偏航的最小和最大程度。测试手势的最大和最小位移分别为10 cm和150 cm。

图8显示了准确性的累积密度函数（CDF），这是计算出的分位数和实际位移之间的差异。我们的实验结果表明，我们的方法能够成功识别人类手势。我们计算成功的识别率

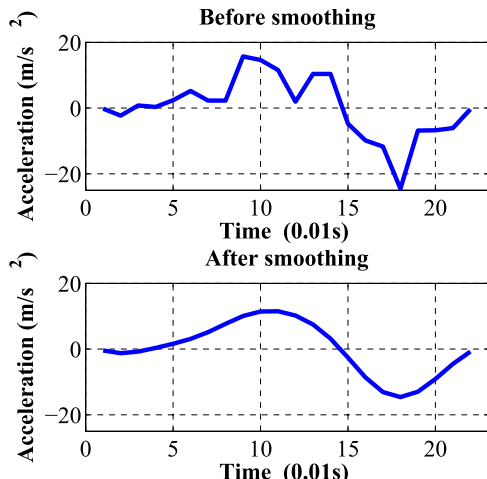


图6。平滑前后。图7。测试的40个手势。

授权许可使用限制为：南卡大学。从IEEE Xplore 下载了5月19日，20125年5月6:47:57 UTC。适用限制

作为整个经过测试手势的数量的成功识别时间的数量。如何识别手势是通过等式 (25) 计算的。实验结果表明，成功的识别率可以达到100%。实验结果显示在图1和图2中。8a和8d。我们可以看到，平均精度约为0:07 m。通过使用改进方法1和2，平均精度可以达到0:06 m。因此，平均准确性可以提高约15%。

为了调查哪种改进方法最多，我们测试了20轮具有较大振幅的手势，另外20轮手势分别具有幅度较小的手势。实验结果显示在图1和图2中。8b和8e以及无花果。8c和8f。我们发现，对于具有较大幅度的吉斯特尔，当使用两种改进方法时，跟踪精度是最好的。对于振幅较小的手势，改进方法1是最好的。原因是以下内容。对于改进方法2，我们使用的相关性和限制

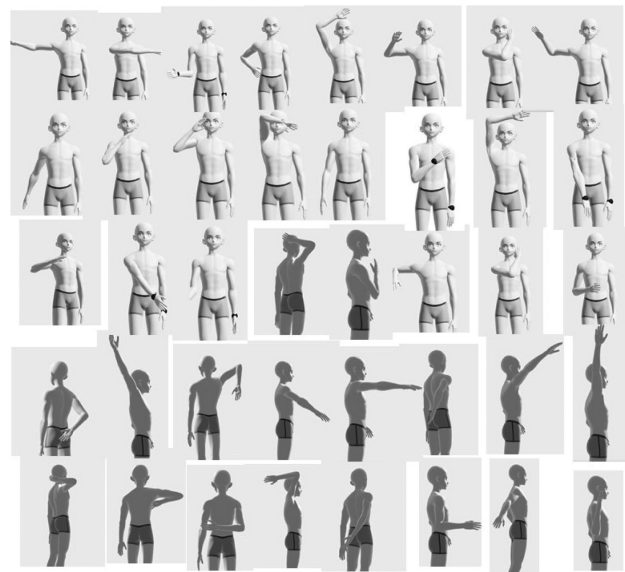


图7。测试的40个手势。

TABLE 2
Gesture Range

	Minimum value	Maximum value
Roll	-60°	180°
Pitch	-90°	145°
Yaw	-90°	145°
Displacement	10cm	150cm

body parts to avoid some abnormal calculated results beyond a certain limited range. However, the gestures with small amplitude usually will not go beyond this limitation. Therefore, in real application, we suggest using both the improvement methods. But in some scenario where only small human motions occur, we may just use the improvement method 1.

When more sensors are placed in the human joints or the sensors are placed on other parts of the body, we can recognize more complicate gestures.

4.5 Results of the Same Gestures With Different Amplitude

In this subsection, we will investigate how our algorithm can recognize the same gestures with different amplitude. We performed 20 rounds of test. In each round of test, we tested a certain gesture with two different amplitude. Each gesture is repeated twice. Fig. 9 is an example of such gesture. Fig. 9 shows the human gesture waving hand to the right. A, B and C are three wearable sensors. The solid line represents the real position of the human body, while the dashed line is the estimated position by our algorithm.

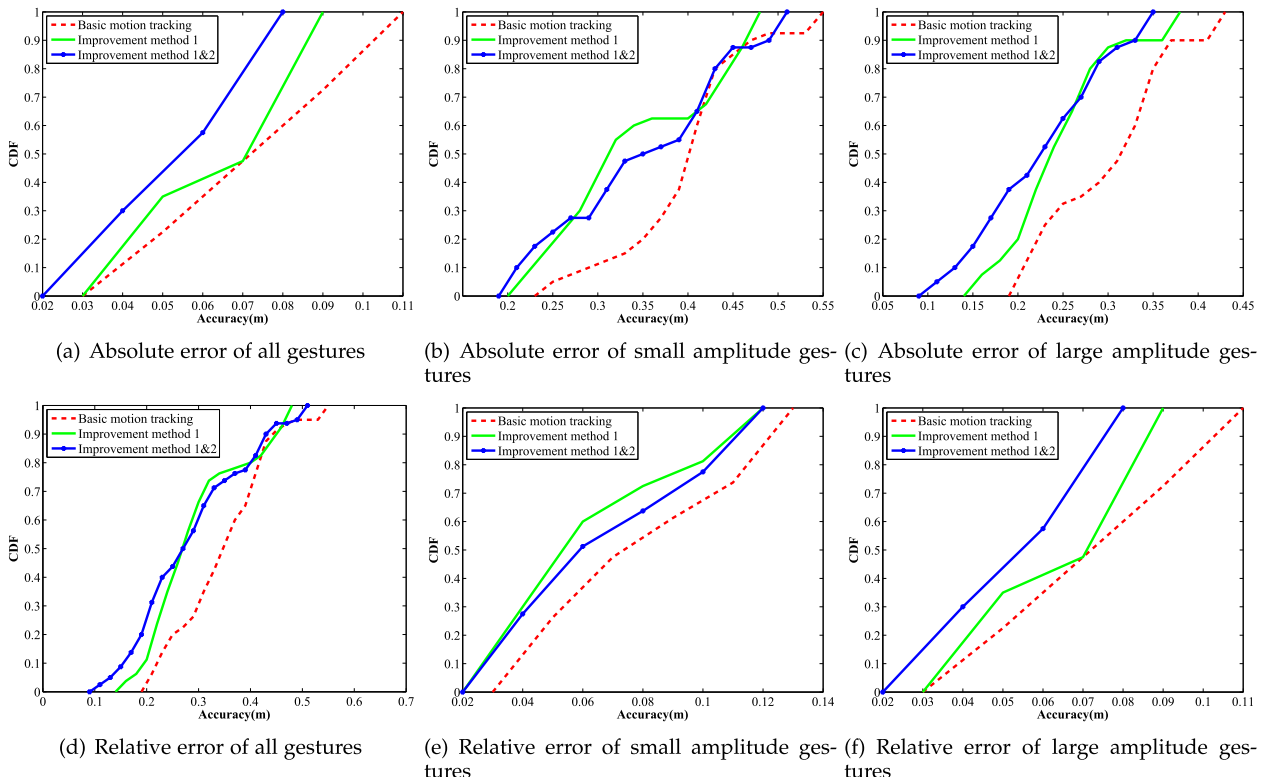


Fig. 8. Accuracy of the motion tracking.

TABLE 3
Comparison of Different Gesture Amplitude

Gesture type	Xu's work [32]	Our system
Small amplitude	95.6%	100%
Both small and large amplitude	40%	100%

Our experiment results show that the successfully recognition rates of the gesture with large and small amplitude are both 100%. Therefore, our algorithm is able to successfully and comprehensively recognize the same gestures with different amplitude.

4.6 Comparisons With Other Algorithms

Our approach in gesture recognition is not limited by the predefined gestures. But in order to conveniently compare our algorithm with traditional algorithms, in this subsection, for the performance metric, we use the recognition rate instead of the previous performance metric accuracy.

The baselines we compared are listed below.

- Xu's work [32]. It is an automatic gesture segmentation algorithm to identify individual gestures in a sequence. It is able to extract a basic feature based on sign sequence of gesture acceleration. This method reduces hundreds of data values of a single gesture to a gesture code of 8 numbers. Finally, the gesture is recognized by comparing the gesture code with the stored templates.
- Cerqueira's work [60]. They used kinematic data and machine learning tools to recognize human upper body postures. The configuration that presented the

表2手势范
围

	Minimum value	Maximum value
Roll	-60°	180°
Pitch	-90°	145°
Yaw	-90°	145°
Displacement	10cm	150cm

身体部位以避免某些异常计算的结果超出一定有限的范围。但是，幅度较小的手势通常不会超出此限制。因此，在实际应用中，我们建议使用这两种改进方法。但是，在某些情况下，只有小动作发生的情况，我们可能只使用改进方法1。

当将更多的传感器放置在人体关节中或将传感器放置在人体其他部位时，我们可以使手势更复杂。

4.5具有不同振幅的相同手势的结果

在本小节中，我们将研究我们的算法如何以不同的幅度识别相同的手势。我们进行了20轮测试。在每一轮测试中，我们都以两个不同的振幅测试了一定的手势。每个手势重复两次。图9是这样的示例。图9显示了人类的手势向右挥舞着手。A, B和C是三个可穿戴传感器。实线代表人体的真实位置，而虚线是我们算法的估计位置。

表3不同手势振幅的比较

Gesture type	Xu's work [32]	Our system
Small amplitude	95.6%	100%
Both small and large amplitude	40%	100%

我们的实验结果表明，大小幅度的成功识别率均为100%。因此，我们的算法能够以不同的幅度取得成功，全面地识别相同的手势。

4.6与其他算法进行比较

我们在手势识别方面的算法不受预定的手势的限制。但是，为了方便地将我们的算法与传统算法进行比较，在此基本中，对于性能指标，我们使用识别率，而不是先前的性能指标准确性。

我们比较的基准在下面列出。

- Xu的工作[32]。它是一种自动手势分段算法，可以识别序列中的单个手势。它能够根据手势加速度的符号序列提取基本功能。此方法将单个手势的数百个数据值减少到8个数字的手势代码。最后，通过将手势代码与存储的模板进行比较，可以识别手势。
- Cerqueira的作品[60]。他们使用运动学数据和机器学习工具来识别人类的上身姿势。提出的配置

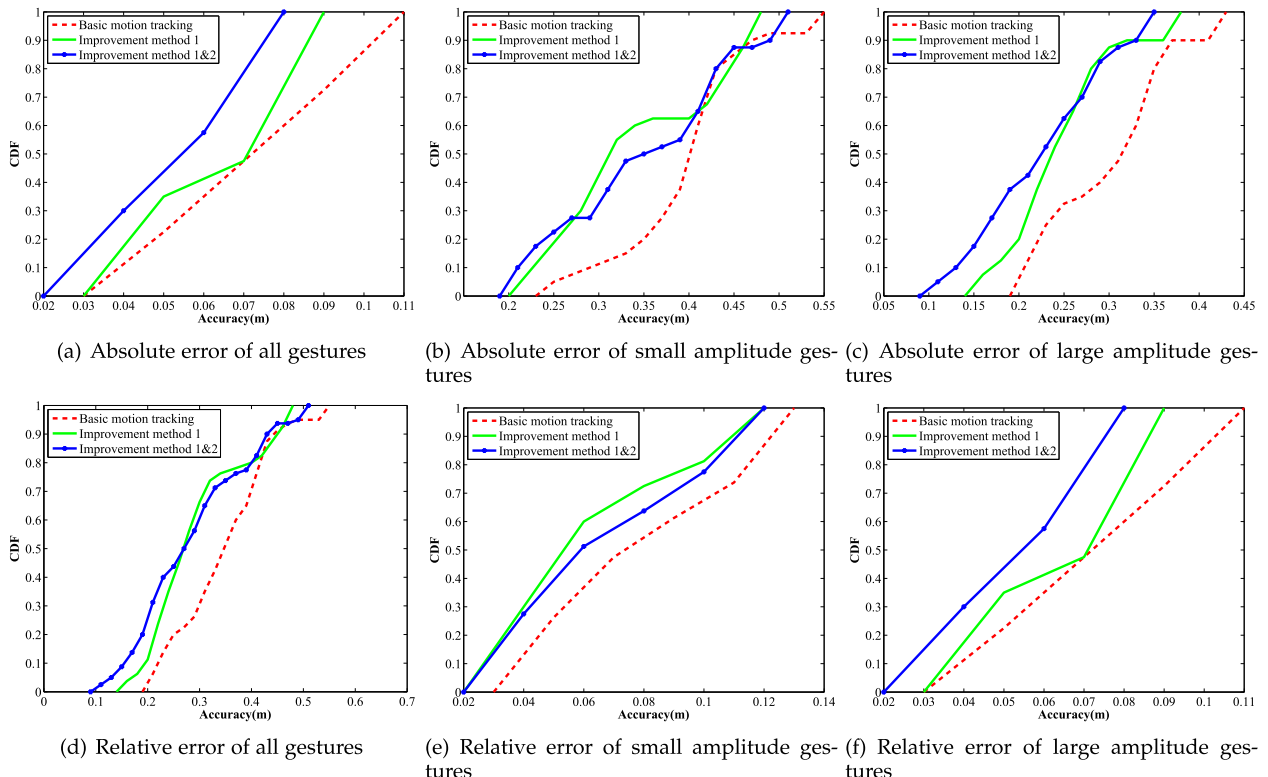


图8。运动跟踪的准确性。

授权许可使用限制为：南卡大学。从IEEE Xplore 下载了5月19日，20125年5月6:47:57 UTC。适用限制。

。

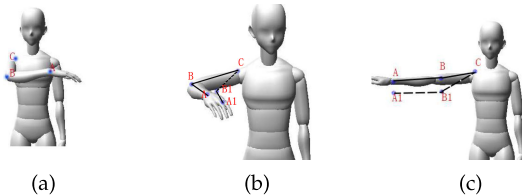


Fig. 9. The gesture is waving hand to the right. The solid line represents the real position of the human body, while the dashed line is the estimated position by our algorithm. (a) is initial position. (b) is the motion with small amplitude. (c) is the motion with large amplitude.

best results was a quadratic SVM classifier, with a Z-score normalization and the mRMR as dimensionality reduction algorithm.

- Kang's work [61]. They collected real time data from an IMU sensor attached to wrist and head of sport participants and used the decision tree-based classification scheme.
- Le's work [62]. It used a wearable device embedded with accelerometer and gyroscope sensors to recognize human hand gesture. It gave the best result when using Random Forests.
- Gochoo's work [52]. They employed a low-resolution infrared sensor-based wireless sensor network (WSN) and used a deep convolutional neural network (DCNN) to recognize yoga postures.
- Elforaici's work [63]. They leveraged CNN and SVM to recognize gestures using an RGB-D camera.
- Banos's work [64]. They presented an alternate approach based on transfer learning to opportunistically train new unseen or target sensor systems from sensor systems.
- Gibran's work [65]. They introduced a new benchmark dataset named IPN Hand with sufficient size, variety, and real-world elements. It utilized a 3D-CNN model in recognition.

Regarding to the tested gestures, we refer to the definition from Xu's work [32] and expanded to 40 different gestures including both large and small amplitude (referred to the definition in Equation (22)). The tested gestures are shown in Fig. 7. The detail setting is explained in Section 4.4. Experimental results show that, when recognizing the gestures with small amplitude, both our algorithm and Xu's algorithm can have high recognition rate. Our method outperformed Xu's algorithm by 4.4%. However, when taking both large and small amplitude gestures into account, the

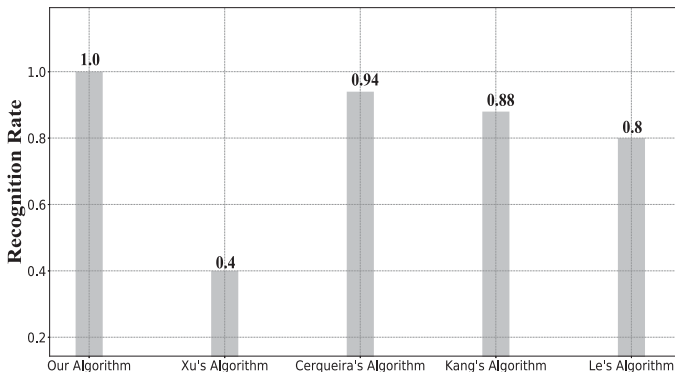


Fig. 10. Comparison with algorithms based on IMU data.

Authorized licensed use limited to: NANKAI UNIVERSITY. Downloaded on May 19, 2025 at 06:47:57 UTC from IEEE Xplore. Restrictions apply.

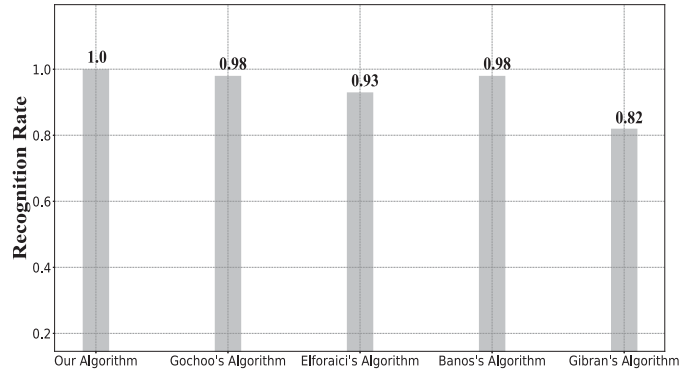


Fig. 11. Comparison with algorithms based on non-IMU data.

successful recognition rate of traditional Xu's work is reduced to 40%. It is noted that the successful recognition rate of our algorithm can still reach 100%, as Fig. 10 shows.

We further compare our algorithms with the baseline algorithms using IMU data. As shown in Fig. 10, our algorithm outperforms traditional Xu's algorithm, Cerqueira's algorithm [60], Kang's algorithm and Le's algorithm by 60%, 6%, 12% and 20%, respectively.

On the other hand, we compare our algorithms with the baseline algorithms using non IMU data. As shown in Fig. 11, our algorithm outperforms Gochoo's work [52], Elforaici's work [63], Bano's algorithm, Gibran's algorithm by 2%, 7%, 2% and 18%, respectively.

To sum up, although machine learning algorithms may have a high recognition rate, our algorithms still outperform them. Specifically, our algorithms do not require training in advance and are not limited by the predefined gestures, which can not be avoided by the machine learning algorithms.

4.7 System Latency

our system mainly contains the steps of data transmission, data processing and noise reductions. The latter two algorithms are implemented in our computer system with an Intel i5-3470K CPU and 8 GB RAM. Their running time can be negligible since it is too short and may vary with different computing systems. Therefore, the total latency is mainly determined by the transmission time, which depends on how much time for each sensor transmit its sensing data back to the server and how many data used in our tracking algorithm. In our setting, each sensor takes 10ms to transmit a packet. We will calculate its location after receiving 80 such packets. Therefore, the total latency is about $80 * 10 = 800ms = 0.8s$.

5 CONCLUSION

In this paper, we propose to exploit the sensing data from the wearable IMU devices to human body gesture recognition. Compared with traditional gesture recognition algorithms which require training, our approach does not have such requirement. We comprehensively study the sensing data, and propose various algorithms to refine the hardware linear distortion, eliminate the impact of the gravity, eliminate the hardware differences and effectively utilize the correlation and limitation among body parts to improve the

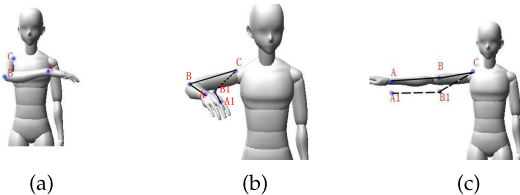


图9。手势向右挥舞。实线代表人体的真实位置，而虚线是我们算法所估算的位置。（a）是初始位置。（b）是振幅较小的运动。（c）是具有较大振幅的运动。

最佳结果是二次SVM分类器，具有z得分归一化，MR作为维数还原算法。

- 康的作品[61]。他们从腕部和运动参与者负责人的IMU传感器中收集了实时数据，并使用了基于决策树的分类方案。
- LE的工作[62]。它使用嵌入加速度计和陀螺仪传感器的可穿戴设备来认可人体手势。使用随机森林时，它给出了最好的结果。
- Gochoo的工作[52]。他们采用了基于低分辨率的红外传感器无线传感器网络（WSN），并使用深度卷积神经网络（DCNN）来识别瑜伽姿势。
- Elforaici的工作[63]。他们利用CNN和SVM使用RGB-D摄像头识别手势。
- Banos的工作[64]。他们提出了一种基于转移学习的方式，从传感器系统培训了新的看不见或目标传感器系统。
- Gibran的工作[65]。他们引入了一个名为IPN手的新基准数据集，其尺寸，品种和现实世界中的元素。它在识别中使用了3D-CNN模型。

关于测试的手势，我们指的是Xu工作[32]的定义，并扩展到40种不同的镜头，包括大小幅度（指方程式（22）中的定义）。测试的手势如图7所示。细节设置在第4.4节中说明。实验结果表明，当识别幅度较小的GES含量时，我们的算法和XU的算法都可以具有很高的识别率。我们的方法将XU的算法超过4: 4%。但是，当考虑大小振幅手势时，

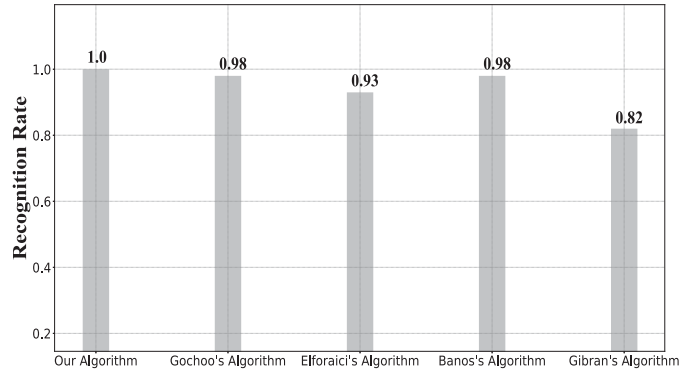


图11。基于非IMU数据的算法进行比较。

传统XU工作的成功认可率降低到40%。值得注意的是，如图10所示，我们算法的成功识别率仍然可以达到100%。

我们进一步将算法与使用IMU数据的基线算法进行了比较。如图10所示，我们的算法 - 远高于传统的Xu算法，Cerqueira的算法[60]，Kang's算法和LE's算法分别为60%，6%，12%和20%。

另一方面，我们使用非IMU数据将算法与基线算法进行比较。如图11所示，我们的算法表现优于Gochoo的作品[52]，Elforaici的作品[63]，Bano的算法，Gibran的算法分别为2%，7%，2%和18%。

总而言之，尽管机器学习算法可能具有很高的识别率，但我们的算法仍然超过它们。具体而言，我们的算法不需要事先培训，也不需要受到预定的手势的限制，这是无法通过机器学习算法避免的。

4.7 系统延迟

我们的系统主要包含数据传输，数据处理和减少噪声的步骤。后两个算法在我们的计算机系统中使用Intel I5-3470K CPU和8 GB RAM实现。他们的运行时间可以忽略不计，因为它太短了，并且可能随不同的计算系统而变化。因此，总延迟主要取决于传输时间，这取决于每个传感器的时间将其传感数据传输回服务器以及在我们的跟踪算法中使用多少数据。在我们的环境中，每个传感器需要10毫秒来传输数据包。我们将在收到80个这样的数据包后计算其位置。因此，总延迟约为 $80 * 10 = 800\text{ms} = 0: 8\text{s}$ 。

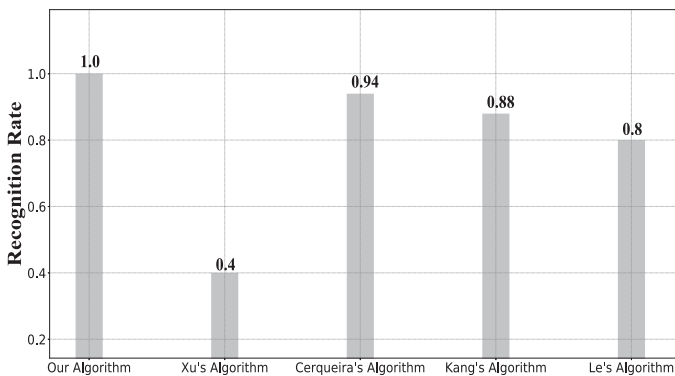


图10。基于IMU数据的算法比较。

授权许可使用限制为：南卡大学。从IEEE Xplore 下载了5月19日，20125年5月6:47:57 UTC。适用限制

身体部位之间的关系和局限性

rove
。

tracking accuracy dramatically. As such, we can accurately recognize the human body gesture and track body motion in real time.

Experimental results have shown that our approach is able to successfully recognize the human gestures. The tracking accuracy of human body motion is about $0.06m$ and the recognition rate is 100%. Furthermore, our approach can recognize the same gestures with different amplitudes. Our algorithm is easily applied to recognize many complicated gestures, if more sensors are deployed on the other part of the body.

The future work is as follows. We will test different human body gestures in different environments. Moreover, more comprehensive algorithms to improve the tracking accuracy can be further investigated.

REFERENCES

- [1] L. E. Sucar, F. Orihueta-Espina, R. L. Velazquez, D. J. Reinkensmeyer, R. Leder, and J. Hernández-Franco, "Gesture therapy: An upper limb virtual reality-based motor rehabilitation platform," *IEEE Trans. Neural Syst. Rehabil. Eng.*, vol. 22, no. 3, pp. 634–643, May 2014.
- [2] Y. Liu, Y. Yin, and S. Zhang, "Hand gesture recognition based on HU moments in interaction of virtual reality," in *Proc. 4th Int. Conf. Intell. Hum.-Mach. Syst. Cybern.*, 2012, pp. 145–148.
- [3] Q. Wan, Y. Li, C. Li, and R. Pal, "Gesture recognition for smart home applications using portable radar sensors," in *Proc. 36th Annu. Int. Conf. IEEE Eng. Med. Biol. Soc.*, 2014, pp. 6414–6417.
- [4] K. Bouchard, A. Bouzouane, and B. Bouchard, "Gesture recognition in smart home using passive RFID technology," in *Proc. 7th Int. Conf. Pervasive Technol. Related Assistive Environ.*, 2014, pp. 1–8.
- [5] J. Zeng, Y. Sun, and F. Wang, "A natural hand gesture system for intelligent human-computer interaction and medical assistance," in *Proc. 3rd Glob. Congr. Intell. Syst.*, 2012, pp. 382–385.
- [6] Y. Zhang, J. Zhang, and Y. Luo, "A novel intelligent wheelchair control system based on hand gesture recognition," in *Proc. IEEE/ICME Int. Conf. Complex Med. Eng.*, 2011, pp. 334–339.
- [7] J. Suarez and R. R. Murphy, "Hand gesture recognition with depth images: A review," in *Proc. 21st IEEE Int. Symp. Robot Hum. Interactive Commun.*, 2012, pp. 411–417.
- [8] A. Arbabian, S. Callender, S. Kang, M. Rangwala, and A. M. Niknejad, "A 94 GHz mm-wave-to-baseband pulsed-radar transceiver with applications in imaging and gesture recognition," *IEEE J. Solid-State Circuits*, vol. 48, no. 4, pp. 1055–1071, Apr. 2013.
- [9] W. Wang, A. X. Liu, M. Shahzad, K. Ling, and S. Lu, "Device-free human activity recognition using commercial Wi-fi devices," *IEEE J. Selected Areas Commun.*, vol. 35, no. 5, pp. 1118–1131, May 2017.
- [10] W. He, K. Wu, Y. Zou, and Z. Ming, "WiG: WiFi-based gesture recognition system," in *Proc. 24th Int. Conf. Comput. Commun. Netw.*, 2015, pp. 1–7.
- [11] J. Yang, H. Zou, Y. Zhou, and L. Xie, "Learning gestures from Wifi: A Siamese recurrent convolutional architecture," *IEEE Internet Things J.*, vol. 6, no. 6, pp. 10763–10772, Dec. 2019.
- [12] Y. Wu, K. Chen, and C. Fu, "Natural gesture modeling and recognition approach based on joint movements and arm orientations," *IEEE Sensors J.*, vol. 16, no. 21, pp. 7753–7761, Nov. 2016.
- [13] S.-O. Shin, D. Kim, and Y.-H. Seo, "Controlling mobile robot using IMU and EMG sensor-based gesture recognition," in *Proc. 9th Int. Conf. Broadband Wirel. Comput., Commun. Appl.*, 2014, pp. 554–557.
- [14] O. Sidek and M. A. Hadi, "Wireless gesture recognition system using MEMS accelerometer," in *Proc. Int. Symp. Technol. Manage. Emerg. Technol.*, 2014, pp. 444–447.
- [15] H. Gunes and M. Piccardi, "Bi-modal emotion recognition from expressive face and body gestures," *J. Netw. Comput. Appl.*, vol. 30, no. 4, pp. 1334–1345, 2007.
- [16] C.-F. Juang and P.-H. Wang, "An interval type-2 neural fuzzy classifier learned through soft margin minimization and its human posture classification application," *IEEE Trans. Fuzzy Syst.*, vol. 23, no. 5, pp. 1474–1487, Oct. 2015.
- [17] C.-H. Ling, C.-W. Lin, C.-W. Su, Y.-S. Chen, and H.-Y. M. Liao, "Virtual contour guided video object inpainting using posture mapping and retrieval," *IEEE Trans. Multimedia*, vol. 13, no. 2, pp. 292–302, Apr. 2011.
- [18] C.-F. Juang, C.-M. Chang, J.-R. Wu, and D. Lee, "Computer vision-based human body segmentation and posture estimation," *IEEE Trans. Syst., Man, Cybern.-Part A: Syst. Hum.*, vol. 39, no. 1, pp. 119–133, Jan. 2009.
- [19] E. Ohn-Bar and M. M. Trivedi, "Hand gesture recognition in real time for automotive interfaces: A multimodal vision-based approach and evaluations," *IEEE Trans. Intell. Transp. Syst.*, vol. 15, no. 6, pp. 2368–2377, Dec. 2014.
- [20] D. Brulin, Y. Benerezeth, and E. Courtial, "Posture recognition based on fuzzy logic for home monitoring of the elderly," *IEEE Trans. Inf. Technol. Biomed.*, vol. 16, no. 5, pp. 974–982, Sep. 2012.
- [21] Z. Ren, J. Yuan, J. Meng, and Z. Zhang, "Robust part-based hand gesture recognition using Kinect sensor," *IEEE Trans. Multimedia*, vol. 15, no. 5, pp. 1110–1120, Aug. 2013.
- [22] Z. Ju, X. Ji, J. Li, and H. Liu, "An integrative framework of human hand gesture segmentation for human-robot interaction," *IEEE Syst. J.*, vol. 11, no. 3, pp. 1326–1336, Sep. 2017.
- [23] K. N. Krisandria, B. S. B. Dewantara, and D. Pramadihanto, "Hog-based hand gesture recognition using Kinect," in *Proc. Int. Electron. Symp.*, 2019, pp. 254–259.
- [24] A. Dzikri and D. E. Kurniawan, "Hand gesture recognition for game 3D object using the leap motion controller with backpropagation method," in *Proc. Int. Conf. Appl. Eng.*, 2018, pp. 1–5.
- [25] L. Shao, "Hand movement and gesture recognition using leap motion controller," Stanford Univ., Stanford, CA, USA, Rep. EE267, 2016.
- [26] W. Lu, Z. Tong, and J. Chu, "Dynamic hand gesture recognition with leap motion controller," *IEEE Signal Process. Lett.*, vol. 23, no. 9, pp. 1188–1192, Sep. 2016.
- [27] J. Wang, L. Zhang, C. Wang, X. Ma, Q. Gao, and B. Lin, "Device-free human gesture recognition with generative adversarial networks," *IEEE Internet Things J.*, vol. 7, no. 8, pp. 7678–7688, Aug. 2020.
- [28] S. H. Chae and S. Chung, "Blind interference alignment for a class of K-user line-of-sight interference channels," *IEEE Trans. Commun.*, vol. 60, no. 5, pp. 1177–1181, May 2012.
- [29] F. Adib, Z. Kabelac, D. Katabi, and R. C. Miller, "3D tracking via body radio reflections," in *Proc. 11th USENIX Symp. Netw. Syst. Des. Implementation*, 2014, pp. 317–329.
- [30] S. Palipana, D. Salami, L. A. Leiva, and S. Sigg, "Pantomime: Mid-air gesture recognition with sparse millimeter-wave radar point clouds," *Proc. ACM Conf. Interactive, Mobile, Wearable Ubiquitous Technol.*, vol. 5, no. 1, 2021, pp. 1–27.
- [31] Y. Zheng et al., "Zero-effort cross-domain gesture recognition with Wi-Fi," in *Proc. 17th Annu. Int. Conf. Mobile Syst., Appl. Serv.*, 2019, pp. 313–325.
- [32] R. Xu, S. Zhou, and W. J. Li, "MEMS accelerometer based non-specific-user hand gesture recognition," *IEEE Sensors J.*, vol. 12, no. 5, pp. 1166–1173, May 2012.
- [33] W. Zheng and D. Zhang, "Handbutton: Gesture recognition of transceiver-free object by using wireless networks," in *Proc. IEEE Int. Conf. Commun.*, 2015, pp. 6640–6645.
- [34] C. Zhang, C.-F. Lai, Y.-H. Lai, Z.-W. Wu, and H.-C. Chao, "An inferential real-time falling posture reconstruction for internet of healthcare things," *J. Netw. Comput. Appl.*, vol. 89, pp. 86–95, 2017.
- [35] J. M. Allen, P. K. Asselin, and R. Foulds, "American sign language finger spelling recognition system," in *Proc. 29th Annu. Proc. Bioeng. Conf.*, 2003, pp. 285–286.
- [36] S. P. Won, W. Melek, and F. Golnaraghi, "A fastened bolt tracking system for a hand-held tool using an inertial measurement unit and a triaxial magnetometer," in *Proc. 35th Annu. Conf. IEEE Ind. Electron.*, 2009, pp. 2703–2708.
- [37] H. P. Gupta, H. S. Chudgar, S. Mukherjee, T. Dutta, and K. Sharma, "A continuous hand gestures recognition technique for human-machine interaction using accelerometer and gyroscope sensors," *IEEE Sensors J.*, vol. 16, no. 16, pp. 6425–6432, Aug. 2016.
- [38] X. Yun and E. R. Bachmann, "Design, implementation, and experimental results of a Quaternion-based Kalman filter for human body motion tracking," *IEEE Trans. Robot.*, vol. 22, no. 6, pp. 1216–1227, Dec. 2006.
- [39] H. Watanabe and T. Terada, "Improving ultrasound-based gesture recognition using a partially shielded single microphone," in *Proc. 2018 ACM Int. Symp. Wearable Comput.*, 2018, pp. 9–16.

急剧跟踪准确性。因此，我们可以实时准确地识别人体的手势和跟踪身体运动。

实验结果表明，我们的方法能够成功识别人类的手势。人体运动的跟踪精度约为0: 06m，识别率为100%。此外，我们的方法可以识别具有不同振幅的相同手势。如果在身体的另一部分部署了更多的传感器，我们的算法很容易被应用以识别许多符合符合的手势。

未来的工作如下。我们将在不同环境中测试不同的人体手势。此外，可以进一步研究更全面的算法以提高跟踪精度。

参考

- [1] L. E. Sucar, F. Orihueta-Espina, R. L. Velazquez, D. J. Reinkensmeier, R. Leder and J. Hernández-Franco, “手势疗法：上肢虚拟现实实现运动康复平台”，*IEEE EEE Trans. 神经系统。康复。Eng.*，卷。22，否。第3卷，第634–643页，2014年5月。[2] Y. Liu, Y. Yin and S. Zhang, “基于虚拟现实相互作用的HU时刻的手势识别”，《Proc.》。第四英特。conf. Intell. 嗡嗡声 - 马赫。系统。Cybern.，2012年，第145–148页。[3] Q. Wan, Y. Li, C. Li and R. Pal, “使用便携式雷达传感器对智能家庭应用的手势识别”，载于Proc. 第36 Annu. int. conf. IEEE ENG. 医学生物。Soc.，2014年，第6414–6417页。[4] K. Bouchard, A. Bouzouane and B. Bouchard, “使用被动RFID技术在智能家庭中的手势认可”，Proc. 第七国际conf. 普遍的技术。相关辅助环境，2014年，第1-8页。[5] J. Zeng, Y. Sun and F. Wang, “用于智能人机互动和医疗援助的自然手势系统”，《Proc.》。第三个地球。恭喜。Intell. Syst.，2012年，第382–385页。[6] Y. Zhang, J. Zhang and Y. Luo, “基于手势识别的新型智能轮椅控制系统”，*IEEE/ ICME int. conf. 复杂的医学。Eng.*，2011年，第334–339页。[7] J. Suarez and R. R. Murphy, “带有深度图像的手势识别：评论”，《Proc.》。21st IEEE INT. SYMP. 机器人嗡嗡作响。Interactive Commun.，2012年，第411–417页。[8] A. Arbabian, S. Callender, S. Kang, M. Rangwala and A. M. Niknejad, “94 GHz mm-Wave-wave-Base-Baseband-Baseband脉冲脉冲 - 雷达 - 雷达式transceiver，并在成像和手势识别中应用”，48，不。第4页，第1055–1071页，2013年4月。[9] W. Wang, A. X. Liu, M. Shahzad, K. Ling and S. Lu, “使用商业Wi-Fi fices使用商业Wi-Fi fices识别设备的无人工活动识别”，*IEEE J. Selection J. Selection J. Selection J. Selection*。35, 不。5, 第1118–1131页, 2017年5月。[10] W. He, K. Wu, Y. Zou and Z. Ming, “假发：基于WiFi的手势识别系统”，载于Proc. 第24英特。conf. 计算。社区。Netw.，2015年，第1-7页。[11] J. Yang, H. Zou, Y. Zhou and L. Xie, “从Wifif中学习手势：暹罗经常性卷积建筑”，*IEEE Inter-Nethings Things J.*, Vol. 6, 不。6, 第10763–10772页, 2019年12月。[12] Y. Wu, K. Chen and C. Fu, “基于关节运动和手臂方向的自然手势建模和化合物方法”，*IEEE Sensors J.*, 第1卷。16, 不。21, 第7753–7761页, 2016年11月。[13] S.-O. Shin, D. Kim and Y.-H. SEO, “使用IMU和基于EMG传感器的手势识别控制移动机器人”，第9个国际conf. 宽带小路。计算。社区。Appl.，2014年，第554–557页。[14] O. Sidek and M. A. Hadi, “使用MEMS加速度计的无线手势识别系统”，载于Proc. int. SYMP. 技术。管理。出现。Technol.，2014年，第444–447页。[15] H. Gunes and M. Piccardi, “表达脸和身体手势的双模式情感识别”，*J. Netw. 计算。Appl.*，卷。30, 否。4, 第1334–1345页, 2007年。[16] C.-F. Juang and P.-H. Wang, “通过软边缘最小化及其人类的分类应用学到的间隔2型神经模糊分类器”，*IEEE Trans. 模糊系统*, 卷。23, 否。5, 第1474–1487页, 2015年10月。
- [17] C.-H. Ling, C.-W. Lin, C.-W. Su, Y.-S. Chen and H.-y. M. Liao, “使用姿势映射和检索的虚拟轮廓引导的视频对象介绍”，*IEEE Trans. 多媒体*, 第一卷。13, 否。2, 第292–302页, 2011年4月。[18] C.-F. Juang, C.-M. Chang, J.-R. Wu and D. Lee, “基于计算机的人体细分和姿势估计”，*IEEE Trans. Syst. Man, Cybern. Part A: Syst. 嗡嗡声*, 卷。39, 没有。1, 第119–133页, 2009年1月。[19] E. Ohn-Bar and M. M. Trivedi, “实时识别汽车接口的手势识别：一种基于多模式的视觉方法和评估”，*IEEE Trans. Intell. transp. Syst.*，卷。15, 不。6, 第2368–2377页, 2014年12月。[20] D. Brulin, Y. Benerezeth and E. Courtial, “基于模糊逻辑的姿态认可，用于对老年人进行家庭监控”，*IEEE Trans. inf. 技术。BioMed.*，卷。16, 不。5, 第974–982页, 2012年9月。[21] 多媒体，第一卷。15, 不。5, 第1110–1120页, 2013年8月。[22] Z. Ju, X. Ji, J. Li and H. Liu, “人类手势分割的人类手机相互作用的综合框架”，*IEEE Syst. J.*, 卷11, 不。3, 第1326–1336页, 2017年9月。[23] K. N. Krisandria, B. S. B. Dewantara and D. Pramadihanto, “使用Kinect使用Kinect的“基于Hog的手势识别”，in Proc. int. 电子。Symp.，2019年，第254–259页。[24] A. Dzikri and D. E. Kurniawan, “使用带有背部方法的Leap Motion Controller对游戏3D对象的手势识别”，*Proc. int. conf. 应用。Eng.*，2018年，第1-5页。[25] L. Shao, “使用Leap Motion Controller的手移动和手势识别”，Stanford Univ.，美国加利福尼亚州斯坦福大学，美国，众议员EE267，2016。[26] W. Lu, Z. Tong and J. Chu, “具有Leap Motion Controller的动态手势识别”，*IEEE Signal Process. Lett.*，卷。23, 否。第9页, 第1188–1192页, 2016年9月。[27] J. Wang, L. Zhang, C. Wang, C. Wang, X. Ma, Q. Gao and B. Lin, “设备免费的人类手势识别，具有生成的对抗性网络”，*IEEE Internet Things J.*, 第1卷。7, 不。8, 第7678–7688页, 2020年8月。[28] S. H. Chae and S. Chung, “一类K-用户视线干扰通道的盲干对准”，*IEEE Trans. Commun.*，卷。60, 没有。5, 第1177–1181页, 2012年5月。[29] F. Adib, Z. Kabelac, D. Katabi and R. C. Miller, “通过人体无线电反射的3D跟踪”，《Proc.》。第11 USENIX SEMMP. netw. 系统。des. 实施，2014年，第317–329页。[30] S. Palipana, D. Salami, L. A. Leiva and S. Sigg, “Pantomime：中空气手势识别，具有稀疏的毫米波雷达点云”，*Proc. ACM Conf. 互动，移动，可穿戴无处不在的技术*，第1卷。5, 不。1, 2021, pp. 1-27。[31] Y. Zheng等人，“具有Wi-Fi的零富特性跨域手势识别”，in Proc. 第17安努。int. conf. 移动系统，应用。Serv.，2019年，第313–325页。[32] R. Xu, S. Zhou and W. J. Li, “基于MEMS加速度计的非用用户手势识别”，*IEEE Sensors J.*, Vol. 12, 不。5, 第1166–1173页, 2012年5月。[33] W. Zheng and D. Zhang, “手键：使用无线网络对无收发器对象的手势识别”，《Proc.》。IEEE INT. conf. Commun.，2015年，第6640–6645页。[34] C. Zhang, C.-F. 莱, Y.-H. 莱, Z.-W. 吴 and H.-C. Chao, “医疗互联网事物的推论实时下降姿势重建”，*J. Netw. 计算。Appl.*，卷。89, 第86–95页, 2017年。[35] J. M. Allen, P. K. Asselin and R. Foulds, “美国手语纸拼写识别系统”，载于Proc. 第29 Annu. Proc. 生物英语。Conf.，2003年，第285–286页。[36] S. P. Won, W. Melek and F. Golnaraghi, “使用惯性测量单元和三轴磁力计的手持工具的固定螺栓跟踪系统”，*Proc. 第35 Annu. conf. IEEEInd. Electron.*，2009年，第2703–2708页。[37] H. P. Gupta, H. S. Chudgar, S. Mukherjee, T. Dutta and K. Sharma, “使用加速度计和陀螺仪传感器进行人机交互的连续手势识别技术”，*IEEE Sensors J.*, 第1卷。16, 不。16, 第6425–6432页, 2016年8月。[38] 机器人，卷。22, 否。第6页, 第1216–1227页, 2006年12月。[39] H. Watanabe and T. Terada, “使用部分屏蔽的单个麦克风改善基于超声的GESSTURE识别”，in Proc. 2018 ACM Int. SYMP. 可穿戴计算机，2018年，第9–16页。

- [40] Y. Zhang, T. Gu, C. Luo, V. Kostakos, and A. Seneviratne, "FinDroidHR: Smartwatch gesture input with optical heartrate monitor," in *Proc. ACM Interactive, Mobile, Wearable Ubiquitous Technol.*, 2018, pp. 1–42.
- [41] V. Becker, P. Oldrati, L. Barrios, and G. Soros, "Touchsense: Classifying finger touches and measuring their force with an electromyography armband," in *Proc. ACM Int. Symp. Wearable Comput.*, 2018, pp. 1–8.
- [42] Y. Zhang, Y. Chen, H. Yu, X. Yang, and W. Lu, "Learning effective spatial-temporal features for SEMG armband-based gesture recognition," *IEEE Internet Things J.*, vol. 7, no. 8, pp. 6979–6992, Aug. 2020.
- [43] T. K. Chan, Y. K. Yu, H. C. Kam, and K. H. Wong, "Robust hand gesture input using computer vision, inertial measurement unit (IMU) and flex sensors," in *Proc. IEEE Int. Conf. Mechatronics, Robot. Automat.*, 2018, pp. 95–99.
- [44] Y. Zhang, Y. Yao, and Y. Luo, "An improved HMM/SVM dynamic hand gesture recognition algorithm," in *Proc. Adv. Display Technol. Micro/Nano Opt. Imag. Technol. Appl.*, 2015, pp. 74–80.
- [45] S. Tan and J. Yang, "Fine-grained gesture recognition using WiFi," in *Proc. IEEE Conf. Comput. Commun. Workshops*, 2016, pp. 257–258.
- [46] J. Wang and F. Chuang, "An accelerometer-based digital pen with a trajectory recognition algorithm for handwritten digit and gesture recognition," *IEEE Trans. Electron.*, vol. 59, no. 7, pp. 2998–3007, Jul. 2012.
- [47] G. R. Naik, A. H. Al-Timemy, and H. T. Nguyen, "Transradial amputee gesture classification using an optimal number of SEMG sensors: An approach using ICA clustering," *IEEE Trans. Neural Rehabil. Eng.*, vol. 24, no. 8, pp. 837–846, Aug. 2016.
- [48] C. Zhu and W. Sheng, "Wearable sensor-based hand gesture and daily activity recognition for robot-assisted living," *IEEE Trans. Syst., Man Cybern.-Part A: Syst. Hum.*, vol. 41, no. 3, pp. 569–573, May 2011.
- [49] J. Zhao and R. S. Allison, "Real-time head gesture recognition on head-mounted displays using cascaded hidden Markov models," in *Proc. IEEE Int. Conf. Syst. Man Cybern.*, 2017, pp. 2361–2366.
- [50] J. Wu, L. Sun, and R. Jafari, "A wearable system for recognizing American sign language in real-time using IMU and surface EMG sensors," *IEEE J. Biomed. Health Inform.*, vol. 20, no. 5, pp. 1281–1290, Sep. 2016.
- [51] A. I. Bhuyan and T. C. Mallick, "Gyro-accelerometer based control of a robotic arm using microcontroller," in *Proc. 9th Int. Forum Strategic Technol.*, 2014, pp. 409–413.
- [52] M. Gochoo *et al.*, "Novel IOT-based privacy-preserving yoga posture recognition system using low-resolution infrared sensors and deep learning," *IEEE Internet Things J.*, vol. 6, no. 4, pp. 7192–7200, Aug. 2019.
- [53] K. Choi and H. Liu, "Low pass filter and band pass filter design," in *Problem-Based Learning in Communication Systems Using MATLAB and Simulink*. Hoboken, NJ, USA: Wiley-IEEE Press, 2016, pp. 55–65.
- [54] What is the Difference Between Zero Offset and Zero Drift?. Accessed: Jun. 30, 2021. [Online]. Available: <https://www.sensorsone.com/zero-offset-drift-difference/>
- [55] K. Shoemake, "Animating rotation with Quaternion curves," in *Proc. Conf. Comput. Graph. Interactive Techn.*, 1985, pp. 245–254.
- [56] C. Croarkin and P. Tobias, *NIST/SEMATECH e-Handbook of Statistical Methods*. Gaithersburg, Md., USA: National Institute of Standards and Technology, 2012.
- [57] D. H. Yu, *Natural Boundary Integral Method and Its Applications*. Beijing, China: Sci. Press, 2003.
- [58] Accessed: Jun. 30, 2021. [Online]. Available: <https://www.invensense.com/products/motion-tracking/6-axis/mpu-6050/>
- [59] B. A. Miller and C. Bisdikian, *Bluetooth Revealed: The Insider's Guide to an Open Specification for Global Wireless Communication*. Upper Saddle River, NJ, USA: Prentice Hall PTR, 2001.
- [60] S. M. Cerqueira, L. Moreira, L. Alpoim, A. Siva, and C. P. Santos, "An inertial data-based upper body posture recognition tool: A machine learning study approach," in *Proc. IEEE Int. Conf. Auton. Robot Syst. Competitions (ICARSC)*, 2020, pp. 4–9.
- [61] M.-S. Kang, H.-W. Kang, C. Lee, and K. Moon, "The gesture recognition technology based on IMU sensor for personal active spinning," in *Proc. 20th Int. Conf. Adv. Commun. Technol.*, 2018, pp. 546–552.
- [62] T.-H. Le, T.-H. Tran, and C. Pham, "The Internet-of-Things based hand gestures using wearable sensors for human machine interaction," in *Proc. Int. Conf. Multimedia Anal. Pattern Recognit.*, 2019, pp. 1–6.
- [63] M. E. Amine Elforaici, I. Chaaraoui, W. Bouachir, Y. Ouakrim, and N. Mezghani, "Posture recognition using an RGB-D camera: Exploring 3D body modeling and deep learning approaches," in *Proc. IEEE Life Sci. Conf.*, 2018, pp. 69–72.
- [64] O. Banos *et al.*, "Opportunistic activity recognition in IoT sensor ecosystems via multimodal transfer learning," *Neural Process. Lett.*, vol. 53, pp. 3169–3197, 2021.
- [65] G. Benitez-Garcia, J. Olivares-Mercado, G. Sanchez-Perez, and K. Yanai, "IPN hand: A video dataset and benchmark for real-time continuous hand gesture recognition," in *Proc. 25th Int. Conf. Pattern Recognit.*, 2021, pp. 4340–4347.



Dian Zhang (Member, IEEE) received the PhD degree in computer science and engineering from the Hong Kong University of Science and Technology (HKUST), Hong Kong, in 2010. She was a research assistant professor with the Fok Ying Tung Graduate School, HKUST. She was also an associate professor with Lingnan University, Hong Kong. She is currently an associate professor with Shenzhen university. Her research interests include big data analytics and mobile computing.



Zexiong Liao was born in 1996 in Shanwei City, China. He received the bachelor's degree in aerospace engineering from HuiZhou University in 2018 and the qualification for admission to the master's degree in engineering from Shenzhen University. His research interests include Internet of Things and big data analytics.



Wen Xie was born in 1996 in Jieyang City, China. He received the bachelor's degree in aerospace engineering from the Guangzhou college, South China University of Technology in 2018 and the qualification for admission to the master's degree in engineering from Shenzhen University. His research interests include Internet of Things and big data analytics.



Xiaofeng Wu received the master's degree in computer science and software engineering from Shenzhen University in 2018. Her master's thesis theme is fine-grained and real-time gesture recognition by Using IMU sensors. She is currently with the Shenzhen Research Institute of Big Data, China. Her research interests include Internet of Things, gesture recognition, and deep learning.

[40] ACM Interactive, 移动, 可穿戴无处不在的技术, 2018年, 第1-42页。[41] V. Becker, P. Oldrati, L. Barrios和G. Soros, “触摸: 对纤维的触摸和用电子板臂臂进行分类”, 在Proc中。acm int. SYMP。可穿戴, 2018年, 第1-8页。[42] Y. Zhang, Y. Chen, H. Yu, X. Yang和W. Lu, “学习有效的基于SEMG臂章的手势识别的有效时空 - 时空特征”, IEEE Internet Things J., 第1卷。7, 不。8, 第6979–6992页, 2020年8月。[43] T. K. Chan, Y. K. Yu, H. C. Kam, H. C. Kam和K. H. Wong, “使用计算机视觉, 惯性测量单元 (IMU) 和FLESORS的强大手势输入”, Proc. IEEE INT. conf. 机器人机器人。自动, 2018年, 第95-99页。[44] Y. Zhang, Y. Yao和Y. Luo, “改进的HMM/SVM动态手势识别算法”, 《Proc》。ADV. 显示技术。微/纳米选择。图像。技术。Appl., 2015年, 第74-80页。[45] S. Tan和J. Yang, “使用wifi的细粒度识别”, 载于Proc. IEEE conf. 计算。社区。讲习班, 2016年, 第257–258页。[46] J. Wang和F. Chuang, “基于加速度计的数字笔, 具有轨迹识别算法, 用于手写数字和手势识别”, IEEE Trans. 电子, 卷。59, 没有。7, 第2998–3007页, 2012年7月。[47] G. R. Naik, A. H. Al-Timemy和H. T. Nguyen, “使用最佳数量的SEMG传感器的跨性别截肢手势分类: 使用ICA聚集的方法: IEEE EEEE Trans. 神经康复。Eng., 卷。24, 没有。8, 第837–846页, 2016年8月。[48] C. Zhu和W. Shen g, “基于可穿戴传感器的手势和日常活动的机器人辅助生活识别”, IEEE Trans. Syst., Man Cybern.-Part A: Syst. 哼, 卷。41, 不。第3卷, 第569–573页, 2011年5月。[49] J. Zhao和R. S. Allison, “使用级联的隐藏玛库夫模型在头部安装显示器上的实时头部手势识别”, 《Proc》。IEEE INT. conf. 系统。Man Cybern., 2017年, 第2361–2366页。[50] J. Wu, L. Sun和R. Jafari, “使用IMU和表面EMG传感器实时识别AmeriCan手语的可穿戴系统”, IEEE J. Biomed. 健康信息, 第1卷。20, 没有。5, pp. 1281–1290, 2016年9月。[51] A. I. Bhuyan和T. C. Mall ick, “使用微控制器对机器人臂对基于gyro-accelerometer的控制”, proc. 第9个国际论坛战略技术, 2014年, 第409–413页。[52] M. Gochoo等人, “新型基于IoT的隐私保护瑜伽识别系统, 使用低分辨率红外传感器和深度学习”, IEEE Internet Things J., Vol. 6, 不。第4页, 第7192–7200页, 2019年8月。[53] K. Choi和H. Liu, “低通滤波器和频段传递滤波器设计”, 在使用Mat-Lab和Simulink的通信系统中基于问题的学习中。美国新泽西州霍博肯: Wiley-Ieee出版社, 2016年, 第55-65页。[54] 零偏移与零漂移之间有什么区别? 访问: 2021年6月30日。[在线]。可用: <https://www.sensorsone.com/零offset-drift-difference/> [55] K. Shoemake, “用quaternion曲线进行动画旋转”, in Proc. conf. 计算。图形。互动技术, 1985年, 第245–254页。[56] C. Croarkin和P. Tobias, NIST/Sematech E Handbook的统计方法。美国马里兰州盖瑟斯堡: 国家标准技术研究所, 2012年。[57] D. H. Yu, 自然边界积分方法及其应用。中国北京: 科学。出版社, 2003年。[58] 访问: 2021年6月30日。[在线]。可用: <https://www.invensense.com/products/motion-tracking/6-axis/mpu-6050/> [59] B. A. Miller和C. Bisdikian, 蓝牙揭示: 全球无线通信的开放规格的内部人士指南。美国新泽西州上萨德尔河: Prentice Hall PTR, 2001年。[60] S. M. Cerqueira, L. Meyira, L. Alpoim, A. Siva和C. P. Santos, “一种基于数据的基于数据的上身姿势识别工具: 一种机器学习方法: 一种机器学习方法”, Proc. IEEE INT. conf. 汽车。机器人系统。比赛 (I CARSC), 2020年, 第4-9页。

[61] M.-S. Kang, H.-W. Kang, C. Lee和K. Moon, “基于IMU传感器的个人主动旋转的手势认可技术”, 载于Proc. 20国际conf. ADV. 社区。Technol., 2018年, 第546–552页。[62] T.-H. Le, T.-H. Tran和C. Pham, “使用可穿戴传感器进行人工机器使用的基于贸易的手势”, 载于Proc. int. conf. 多媒体肛门。模式识别., 2019年, 第1-6页。[63] M. E. Amine Elforaici, I. Chaaraoui, W. Bouachir, Y. Uakrim和N. Mezghani, “使用RGB-D相机的姿势识别: 探索3D身体建模和深度学习方法”, Proc. IEEE Life Sci. Conf., 2018年, 第69-72页。[64] O. B anos等人, “通过多模式转移学习, IoT传感器生态系统中的机会活动识别”, 神经过程。Lett., 卷。53, pp. 3169–3197, 2021。[65] G. Ben itez-Garcia, J. Olivares-Mercado, G. Sanchez-Perez和K. Yanai, “IPN Hand: IPN Hand: 视频数据集和实时连续手势识别的视频数据集和基准标准”。25th int. conf. Pat-Tern Wentit., 2021年, 第4340–4347页。



Dian Zhang (IEEE, IEEE成员) 于2010年获得香港科学技术大学 (HKUST) 的计算机科学和工程博士学位。她还是林南大学的副教授, 香港。她目前是深圳大学的副教授。她的研究兴趣包括大数据分析和移动计算。



Zexiong Liao于1996年出生在中国山威市。他于2018年获得了Huizhou University的航空航天工程学士学位, 并获得了深圳大学获得工程硕士学位的资格。他的研究兴趣包括物联网和大数据分析。



Wen Xie于1996年出生在中国的Jieyang City。他于2018年获得广州南方技术大学的广州学院的航空航天工程学士学位, 并获得了深圳大学获得工程硕士学位的资格。他的研究兴趣包括物联网和大数据分析。



小吴 (Xiaofeng Wu) 于2018年获得了深圳大学的计算机科学和软件工程硕士学位。她的硕士学位论文主题是使用IMU传感器的精密和实时的手势。她目前在中国深圳大数据研究所工作。她的研究兴趣包括物联网, 手势识别和深度学习。



Haoran Xie (Senior Member, IEEE) received the PhD degree in computer science from the City University of Hong Kong. He is currently an associate professor with the Department of Computing and Decision Sciences, Lingnan University, Hong Kong. He has authored or coauthored 247 research publications, including 119 journal articles. Among all 119 journal articles, there are 94 SCI/SSCI indexed and 13 SCOPUS indexed. His research interests include artificial intelligence, big data, and educational technology. He

was the recipient of 14 research awards, including the Golden Medal and the Special Award from International Invention Innovation Competition in Canada, and five best paper awards from WI 2020, ICBL 2020, DASFAA 2017, ICBL 2016, and SECOP 2015. He is the editor-in-chief of the *Computers Education: Artificial Intelligence*, an associate editor for the *Array Journal*, *Australasian Journal of Educational Technology*, *Advances in Computational Intelligence*, and the *International Journal of Mobile Learning and Organisation*. He has successfully obtained more than 50 research grants, the total amount of which is more than HK\$27 million. He is a senior member of ACM and a life member of AAAI.



Jiang Xiao received the BSc degree from the Huazhong University of Science and Technology (HUST), Wuhan, China, in 2009 and the PhD degree from Hong Kong University of Science and Technology in 2014. She is currently an associate professor with the School of Computer Science and Technology, HUST. Her research interests include blockchain, distributed computing, wireless indoor localization, and smart sensing. She has directed and participated in many research and development projects and grants from funding agencies such as the National Natural Science Foundation of China (NSFC), Hong Kong Research Grant Council (RGC), Hong Kong Innovation and Technology Commission (ITC), and industries like Huawei, Tencent, and Intel, and has been invited by NSFC in reviewing research projects. She was the recipient of several awards including the CCF-Intel Young Faculty Research Program 2017, Hubei Downlight Program 2018, ACM Wuhan Rising Star Award 2019, and the best paper awards from IEEE ICPADS/GLOBECOM/GPC.



Landu Jiang received the BEng degree in information security engineering from Shanghai Jiao Tong University, the MSc degree in computer science from the University of Nebraska-Lincoln, and the PhD degree with the School of Computer Science, McGill University. He is currently working toward the master's degree (minor) in construction management. His research interests include computer vision, machine learning, smart sensing, wearable and mobile computing, cyber-physical systems, green energy solutions, and online social networks.

▷ For more information on this or any other computing topic, please visit our Digital Library at www.computer.org/csl.



Haoran Xie (IEEE高级成员) 获得了香港城市大学的计算机科学博士学位。他目前是香港林南大学计算与决策科学系的协会教授。他撰写或合着了247个研究出版物，其中包括119篇期刊文章。在所有119篇期刊文章中，有94个SCI/SSCI索引和13个Scopus索引。他的研究兴趣包括人工智能，大数据和教育技术。他



Landu Jiang获得了上海Jiao Tong大学的Information Security Engineering，内布拉斯加州林肯大学的计算机科学学士学位以及麦吉尔大学计算机科学院的博士学位。他目前正在攻读硕士学位（未成年人）。他的研究兴趣包括计算机视觉，机器学习，智能感测，可穿戴和移动计算，网络物理系统，绿色能源解决方案和在线社交网络。

was the recipient of 14 research awards, including the Golden Medal and the Special Award from International Invention Innovation Competition in Canada, and five best paper awards from WI 2020, ICBL 2020, DASFAA 2017, ICB 2016, and SECOP 2015. He is the editor-in-chief of the Computers Education: Artificial Intelligence, an associate editor for the Array Journal, Australasian Journal of Educational Technology, Advances in Computing and Information Systems, and Journal of Educational Technology and International Mobile Learning and Organizational Development. He successfully obtained more than 50 research grants, totaling over 2.7 million Hong Kong dollars. He is a senior member of ACM and a life member of AAAI.

“有关此或任何其他计算主题的更多信息，请访问我们的数字图书馆www.computer.org/cndl。”



Jiang Xiao于2009年获得了中国武汉华盛顿科技大学(HUST)的学士学位，并于2014年获得了香港科学技术大学的博士学位。她目前是计算机科学技术学院的副教授。她的研究兴趣包括区块链，分布式计算，无线室内定位和智能感测。她指导并参加了许多研究和开发项目以及资金的赠款。

诸如中国国家自然科学基金（NSFC），香港研究赠款委员会（RGC），香港创新技术委员会（ITC）等机构以及NSFC邀请NSFC邀请您从事研究项目。她获得了多项奖项的获得者，包括2017年CCF-Intel年轻教师研究计划，2018年Hubei调节计划，ACM Wuhan Rising Star 2019，以及IEEE ICPADS/GLOBECOM/GPC的最佳纸质奖项。